The ubiquitin-like modifier FAT10 is induced in MASLD and impairs the lipid-regulatory activity of PPARα

Ludivine Clavreul, Lucie Bernard, Alexia K Cotte, Nathalie Hennuyer, Cyril Bourouh, Claire Devos, Audrey Helleboid, Joel T Haas, An Verrijken, Céline Gheeraert, et al.

▶ **To cite this version:**

Ludivine Clavreul, Lucie Bernard, Alexia K Cotte, Nathalie Hennuyer, Cyril Bourouh, et al.. The ubiquitin-like modifier FAT10 is induced in MASLD and impairs the lipid-regulatory activity of PPARα. Metabolism, 2024, 151, pp.155720. 10.1016/j.metabol.2023.155720 . hal-04362961

HAL Id: hal-04362961
https://hal.science/hal-04362961

Submitted on 13 Feb 2024

HAL is a multi-disciplinary open access archive for the deposit and dissemination of scientific research documents, whether they are published or not. The documents may come from teaching and research institutions in France or abroad, or from public or private research centers.

L'archive ouverte pluridisciplinaire **HAL**, est destinée au dépôt et à la diffusion de documents scientifiques de niveau recherche, publiés ou non, émanant des établissements d'enseignement et de recherche français ou étrangers, des laboratoires publics ou privés.

The ubiquitin-like modifier FAT10 is induced in MASLD and impairs the lipid regulatory activity of PPARα

Ludivine Clavreul*, Lucie Bernard*, Alexia K. Cotte, Nathalie Hennuyer, Cyril Bourouh, Claire Devos, Audrey Helleboid, Joel T. Haas, An Verrijken, Céline Gheeraert, Bruno Derudas, Loïc Guille, Julie Chevalier, Jérôme Eeckhoute, Emmanuelle Vallez, Emilie Dorchies, Luc Van Gaal, Guillaume Lassailly, Sven Francque, Bart Staels+, Réjane Paumelle+#

* Co-first authors

+ Co-senior authors

Corresponding author: rejane.lestrelin@univ-lille.fr

Highlights:

- FAT10 is upregulated in human and murine MASLD and correlates negatively with *PPARα*
- FAT10 interacts with PPARα in human and mouse hepatocytes
- FAT10 downregulation increases PPARα lipid metabolic activity
- FAT10 overexpression inhibits beneficial PPARα agonist effects on liver steatosis

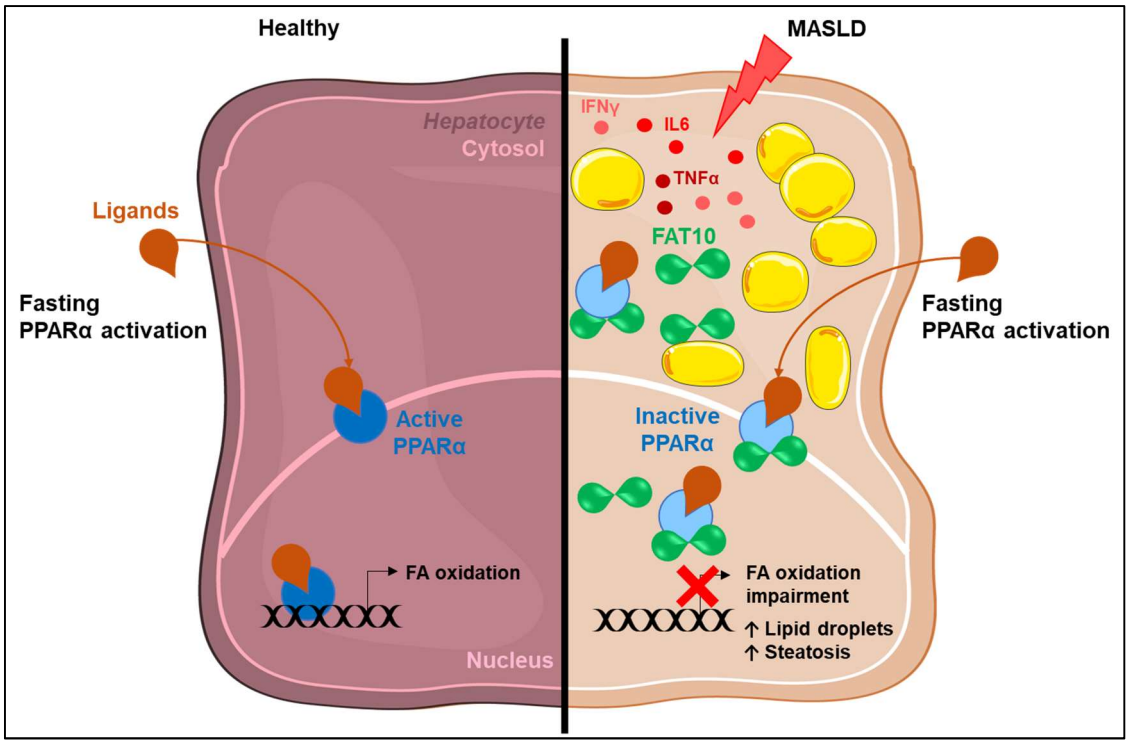

Graphical abstract: The ubiquitin-like modifier FAT10 is induced in MASLD and impairs the lipid regulatory activity of PPARα. In healthy hepatocytes, the transcriptional activity of Peroxisome Proliferator-Activated Receptor α (PPARα) is activated upon fasting by its natural ligands (i.e. fatty acids (FA)) or upon treatment by its synthetic agonist. In response, PPARα activates the transcription of FA oxidation-related genes, hence stimulating lipid metabolism. In Metabolic-dysfunction Associated Steatotic Liver Disease (MASLD), the ubiquitin-like modifier protein human leukocyte antigen-F Adjacent Transcript 10 (FAT10) is induced by pro-inflammatory stimuli (i.e. Interferon γ (IFNγ), Interleukin 6 (IL6) and Tumor Necrosis Factor α (TNFα)). FAT10 then interacts with PPARα, resulting in the inhibition of PPARα activation by its ligands. As a consequence, lipid metabolism and FA oxidation are impaired, and the accumulation of lipid droplets, steatosis and MASLD progression promoted.

The ubiquitin-like modifier FAT10 is induced in MASLD and impairs the lipid-regulatory activity of PPARα

Ludivine Clavreul[1]*, Lucie Bernard[1]*, Alexia K. Cotte[1], Nathalie Hennuyer[1], Cyril Bourouh[1], Claire Devos[1], Audrey Helleboid[1], Joel T. Haas[1], An Verrijken[2,3], Céline Gheeraert[1], Bruno Derudas[1], Loïc Guille[1], Julie Chevalier[1], Jérôme Eeckhoute[1], Emmanuelle Vallez[1], Emilie Dorchies[1], Luc Van Gaal[2,3], Guillaume Lassailly[4], Sven Francque[2,5,6], Bart Staels[1+], Réjane Paumelle[1+#]

1 University of Lille, Inserm, CHU Lille, Institut Pasteur de Lille, U1011, EGID, Boulevard du Professeur Jules Leclercq 59045 Lille France

2 Laboratory of Experimental Medicine and Paediatrics, Faculty of Medicine and Health Sciences, University of Antwerp, 1 B-2610 Antwerp Belgium

3 Department of Endocrinology, Diabetology and Metabolism, Antwerp University Hospital, 1 B-2610 Antwerp Belgium

4 Univ. Lille, Inserm, CHU Lille, U1286 - INFINITE - Institute for Translational Research in Inflammation, 1 place de Verdun 59000 Lille France

5 Department of Gastroenterology and Hepatology, Antwerp University Hospital, 1 B-2610 Antwerp Belgium

6 European Reference Network on Hepatological Diseases (ERN RARE-LIVER), Germany

* Co-first authors

+ Co-senior authors

Corresponding author: rejane.lestrelin@univ-lille.fr

Abstract:

Background and Aims: Peroxisome proliferator-activated receptor α (PPARα) is a key regulator of hepatic lipid metabolism and therefore a promising therapeutic target against Metabolic-dysfunction Associated Steatotic Liver Diseases (MASLD). However, its expression and activity decrease during disease progression and several of its agonists did not achieve sufficient efficiency in clinical trials with, surprisingly, a lack of steatosis improvement. Here, we identified the Human leukocyte antigen-F Adjacent Transcript 10 (FAT10) as an inhibitor of PPARα lipid metabolic activity during MASLD progression.

Approach and Results: *In vivo*, the expression of FAT10 is upregulated in human and murine MASLD livers upon disease progression and correlates negatively with PPARα expression. The increase of FAT10 occurs in hepatocytes in which both proteins interact. FAT10 silencing *in vitro* in hepatocytes increases PPARα target gene expression, promotes fatty acid oxidation and decreases intra-cellular lipid droplet content. In line, FAT10 overexpression in hepatocytes *in vivo* inhibits the lipid regulatory activity of PPARα in response to fasting and agonist treatment in conditions of physiological and pathological hepatic lipid overload.

Conclusions: FAT10 is induced during MASLD development and interacts with PPARα resulting in a decreased lipid metabolic response of PPARα to fasting or agonist treatment. Inhibition of the FAT10-PPARα interaction may provide a means to design potential therapeutic strategies against MASLD.

Keywords: FAT10, UBD, PPARα, MASLD, MASH, Liver

1. Abbreviations

AAV Adeno-Associated Virus

ACAA1 Acetyl-CoA Acyltransferase 1

ACO Acyl-CoA Oxidase

Ad Adenovirus

ANOVA Analysis of variance

CDAA Choline-Deficient diet enriched in cholesterol, fat, glucose and fructose

CPT1α Carnitine Palmitoyltransferase 1 α

FAT10 Human leukocyte antigen-F Adjacent Transcript 10

FATP1 Fatty Acid Transporter 1

GO Gene Ontology

HCC Hepatocellular Carcinoma

HFSC High Fat diet supplemented with Sucrose and Cholesterol

HMGCS2 3-hydroxy-3-methylglutaryl-CoA synthase 2

IF Immunofluorescent

IFNγ Interferon γ

MCD Methionine and Choline-Deficient

MASL Metabolic-dysfunction Associated Steatotic Liver

MASH Metabolic-dysfunction Associated Steatohepatitis

MASLD Metabolic-dysfunction Associated Steatotic Liver Disease

NKT Natural Killer T

NPC Non-Parenchymal Cells

PH Primary Hepatocytes

PLA Proximity Ligation Assay

PPARα Peroxisome Proliferator-Activated Receptor α

SLC27A1 Solute Carrier Family 27 Member 1

TBG Thyroxin-Binding Globulin

TNFα Tumor Necrosis Factor α

UBD Ubiquitin D

2. Introduction

As sedentary lifestyle and high caloric diet become more and more common, the prevalence of Metabolic-dysfunction Associated Steatotic Liver Disease (MASLD), formerly known as Non-Alcoholic Fatty Liver Disease (NAFLD) [1], increases [2]. MASLD covers a spectrum of liver abnormalities starting with, most frequently in obese patients, an accumulation of triglycerides in hepatocytes, called steatosis or MASL (Metabolic-dysfunction Associated Steatotic Liver). Steatosis can evolve upon the development of inflammation and liver cell damage (evidenced by ballooning of hepatocytes) to Metabolic-dysfunction Associated Steatohepatitis (MASH), the more aggressive stage of MASLD [3], formerly referred as Non-Alcoholic Steatohepatitis (NASH) [1]. MASH is a risk factor for the development of clinical hepatic and extra-hepatic disorders, such as cardiovascular diseases, type 2 diabetes, cirrhosis, and hepatocellular carcinoma (HCC) [4,5]. Therefore, molecules targeting a large number of pathways are in development to cure MASLD, but no treatment has been approved so far [6].

Peroxisome Proliferator-Activated Receptors (PPARs), transcription factors belonging to the nuclear receptor family, are amongst the most promising targets to treat MASLD. Within the PPAR family, PPARα, which is highly expressed in the liver, has been shown to modulate MASLD in preclinical animal models [7]. In hepatocytes, PPARα regulates numerous pathways involved in energy homeostasis through the transcriptional regulation of its target genes. PPARα modulates energy metabolism both during physiological nutritional transition states as well as under pathological conditions. Indeed, under fasting conditions, PPARα induces the transcription of genes involved in lipid uptake (Solute Carrier Family 27 Member 1 or Fatty Acid Transporter 1

(*SLC27A1 or FATP1*)), mitochondrial and peroxisomal β-oxidation (Carnitine Palmitoyltransferase 1 (*CPT1α*), Acyl-CoA Oxidase (ACO) and Acetyl-CoA Acyltransferase 1 (*ACAA1*)) and ketogenesis (3-hydroxy-3-methylglutaryl-CoA synthase 2 (*HMGCS2*)) in hepatocytes [8]. In line, PPARα-deficiency in mice promotes the development of obesity and MASLD in response to high fat diet feeding [9]. On the contrary, PPARα activation with selective agonists, such as pemafibrate, prevents diet-induced dyslipidaemia and MASLD development [10–12]. PPARα activation also reduces hepatic inflammation and fibrosis through its transrepressive anti-inflammatory activity [13]. Unfortunately, hepatic PPARα gene expression decreases during MASLD progression [13]. Moreover, although promising effects are observed [15,16], the activation of PPARα with selective or dual agonists in MASLD patients has proven insufficiently effective to induce MASH resolution, with a surprising lack of steatosis improvement. Indeed, the dual PPARα/δ agonist elafibranor (ClinicalTrials.gov NCT02704403) failed in phase 3, and older fibrates have yielded mixed results in MASLD (as reviewed by Pawlak, Lefebvre and Staels, 2015 [7]). A better understanding of the mechanisms modulating PPARα activity in MASLD livers is therefore crucial to evaluate its potential as target for the treatment of the disease.

In the present study, we searched for genes upregulated in MASLD and negatively correlating with PPARα expression to identify novel mechanisms of PPARα modulation during the progression of the disease. Transcriptomic analysis of human livers identified the gene *UBD* (Ubiquitin D, referred as *FAT10* hereinafter) which encodes the Human leukocyte antigen-F Adjacent transcript 10 (FAT10), a protein member of the ubiquitin-like family [17], as a potential candidate. FAT10 is composed of two ubiquitin-like domains linked by a linker and a di-glycine motif at its C-terminal end [18].

This latter motif allows FAT10 to interact covalently with its partners through an enzymatic cascade called FATylation [19]. FATylation can then lead to proteasomal or lysosomal degradation of the FATylated proteins [20]. Under physiological conditions, FAT10 is exclusively expressed in the immune system. However, pro-inflammatory stimuli induce its expression also in other organs like the liver [21]. Here, we identify FAT10 as a modulator of PPARα lipid metabolic activity in hepatocytes induced during the progression of MASLD.

3. Methods

See Supplemental methods for more details.

3.1 Human and liver samples

All patients were consecutively recruited at the Liver Clinic and Obesity Clinic of the Antwerp University Hospital and underwent hepatologic and metabolic work-ups. Exclusion criteria were alcohol consumption > 2 U/day for women and > 3 U/day for men, liver diseases other than MASLD, age < 18 years, liver cirrhosis. For the baseline liver gene expression analysis, patients (N = 205) were selected from the cohort and divided in two groups (no MASH, N = 77 and MASH, N = 128). Of the no MASH patients, 17 had a steatosis score of at least 1 (NAFL) and 60 a steatosis score of 0. Patients' biological parameters are summarized in **Supplementary table 3**. A number of obese MASH patients with paired biopsies at 1 year post-surgery follow-up ("Roux-en-Y" Gastric Bypass (RYGB) N = 15) were also included for gene expression analysis. The study protocol is part of the Hepadip protocol (Belgian registration number B30020071389) and was approved by the Ethical Committee of the Antwerp University Hospital (file 6/25/125). Written informed consent was obtained from all patients in accordance with both the Declarations of Helsinki and Istanbul.

3.2 Animal studies

Wild-type male C57BL/6J mice (8 weeks of age) were purchased from Charles River Laboratories (France). Mice were maintained in pathogen-free environment (12:12 h light/dark cycle, 21 °C-24 °C) with *ad libitum* access to water and food. Littermate animals were randomized by body weight prior to the start of the diet. *In vivo*

experiments were conducted and are described in accordance with the ARRIVE guidelines 2.0.

Mice were fed either with a control diet (CSAA, 16 % kcal fat, 72 % kcal carbohydrates, 12 % kcal protein, SSNIFF Spezialdiäten GmbH, E15668-04) or a choline deficient diet with low methionine level (CDAA, 21 % kcal fat, 58 % kcal carbohydrates, 11 % kcal protein, SSNIFF Spezialdiäten GmbH, E15666-947) enriched with 1 % (by weight) cholesterol and supplemented with a drinking water composed of 55 % of fructose (23.1 g/L, Sigma) and 45 % of glucose (18.9 g/L, Sigma) for 2 or 5 weeks. Then, total liver was taken or mouse primary hepatocytes were isolated from CSAA or CDAA mice using collagenase perfusion as described before [22] to undergo Affymetrix assay.

Mice were fed either a control diet (standard rodent Chow, 5 % kcal fat) or a HFSC (High Fat, Sucrose and Cholesterol) diet (45 % kcal fat, 40 % kcal carbohydrates, 15 % kcal protein, with 1 % (by weight) cholesterol, SAFE diets, France) for 4, 8 and 24 weeks [23].

FAT10 transient overexpression was performed on C57BL/6J wild-type mice (8 weeks of age) by injecting via the tail vein a solution containing 2.5 x 10^8 genome copies (GC) of a control adenovirus (Ad-CTRL) or the adenovirus overexpressing FAT10 (Ad-FAT10) both purchased from Genecust. Four days after adenovirus injections, mice were fasted during 18 h and the liver and blood samples were taken.

Stable FAT10 overexpression in hepatocytes was performed in C57BL/6J wild-type mice (12 weeks of age) by injecting via the tail vein a solution containing 1 x 10^{11} GC of a control or FAT10 overexpressing AAV8 vector driven by a TBG (Thyroxin-Binding

Globulin) promoter (AAV-CTRL and AAV-FAT10) purchased from Polyplus. Mice were fasted 5 h before collecting the liver samples.

Half of the injected mice of each group (Ad-CTRL, Ad-FAT10, AAV-CTRL, AAV-FAT10) were treated by gavage with pemafibrate (1 mpk; Sigma) administered the evening before sacrifice and the morning 5 h before sacrifice. Vehicle (CMC) was given as control to the other mouse group.

All experiments were performed following approval by the Ethics Committee for Animal Experimentation from Nord-Pas de Calais Region (APAFIS #33526-2021092316263268 v4, APAFIS#5746-2016040109244171 and APAFIS#7160-2017040313471173).

3.3 Statistical analysis

All data were expressed as mean ± standard deviation (SD) or standard error of measurement (SEM), as indicated in the legends of each figure. Student's unpaired *t*-test was performed to assess statistical differences between two groups, and comparisons for more than two groups were performed using one-way ANOVA. Finally, differences between two groups under two different factors were examined by a two-way ANOVA. In all analyses, a *p*-value of $p < 0.05$ is considered significant.

4. Results

4.1 FAT10 is elevated in MASH patient livers and correlates negatively with *PPARα* expression

To identify genes potentially modulating the down-regulation of PPARα expression and activity during MASLD progression, hepatic transcriptomic data from a large cohort of obese patients spanning all histological stages of MASH were assessed to identify genes upregulated in livers of MASH patients [14]. Gene Ontology (GO) term pathway analysis (Suppl. Fig. 1A) confirmed previous findings that “PPAR signaling pathways” are dysregulated in MASH vs no-MASH patients, data in line with the down-regulation of *PPARα* upon MASH progression [14]. Differential gene expression analysis comparing no-MASH (N = 77) and MASH (N = 128) patients identified a subset of genes whose expression is induced in MASH livers (Suppl. Fig. 1B). As expected, the expression of genes involved in inflammation, such as *CXCL10* and *CXCL9,* is elevated in the livers of MASH patients [23]. Interestingly, *FAT10* mRNA is two-fold higher in MASH livers, both at the mRNA (Figure 1A,C) as well as at the protein levels as demonstrated by immunofluorescence (IF) analysis (Figure 1B). Interestingly, staining for FAT10 mainly localized in hepatocytes. Moreover, *FAT10* expression positively correlates with the expression of inflammatory genes associated with MASLD severity, such as *IL32*, *CXCL10* and *CXCL9* (Suppl. Fig. 1C) [24], suggesting that FAT10 expression increases in parallel with the inflammation appearing with MASH development.

FAT10 gene expression increases upon disease progression (Figure 1C) and positively correlates with all histological MASLD parameters, *i.e.* steatosis, ballooning and inflammation (Figure 1D) [25]. Moreover, immunofluorescent (IF) staining of

FAT10 on liver biopsies from MASH patients before (M0) and 12 months (M12) after bariatric surgery revealed that FAT10 protein levels decrease upon MASH resolution (Figure 1E). In parallel, *FAT10* gene expression decreases upon MASH resolution (Figure 1E).

Interestingly, *PPARα* expression is restored during MASH regression in these patients [14]. Also, *FAT10* expression correlates negatively with the expression of *PPARα* and its target genes (Figure 1F), such as *HMGCS2* or *ACAA1,* suggesting that *FAT10* upregulation is associated with an impaired lipid metabolism regulation by PPARα.

Taken together, these observations show that *FAT10* gene expression is upregulated in MASH livers and correlates positively with disease severity and negatively with the expression of *PPARα* and its target genes.

4.2 FAT10 is overexpressed in hepatocytes and correlates negatively with PPARα during MASH development in murine livers

FAT10 and PPARα expression levels were analysed in livers of several murine models of MASLD associated with a pronounced hepatic lipid overload. Hepatic *Fat10* gene expression was already induced after two weeks and further increased after 5 weeks of feeding a choline-deficient diet enriched in cholesterol, fat, glucose and fructose (CDAA) compared to the control diet (CSAA) (Figure 2A). Interestingly, a similar increase in *Fat10* mRNA levels is also observed in livers of mice fed a high fat diet supplemented with sucrose and cholesterol (HFSC) [23] (Figure 2A) and of db/db mice fed a methionine and choline-deficient (MCD) diet (data not shown) [26]. These data demonstrate that *Fat10* expression is increased in several murine models of diet-induced MASH.

In the liver, PPARα is highest expressed in hepatocytes in which it plays a crucial role in the regulation of lipid metabolism [8]. Consequently, *Fat10* expression was assessed in primary hepatocytes (PH) *vs* non-parenchymal cells (NPC) isolated from livers of mice after 2 weeks of CDAA diet feeding. Gene expression analysis (Figure 2B) showed that *Fat10* is among the genes induced in PH of CDAA compared to CSAA mice. As expected [27], *Fat10* is expressed in the immune cell-containing NPC fraction, but its expression is not increased in these cells upon CDAA diet feeding (Figure 2B right panel). In line, FAT10 IF staining reveals an increase mainly in hepatocytes in CDAA, but not CSAA-fed mice (Figure 2C). Moreover, *Fat10* mRNA levels correlate negatively with *Pparα* expression (Figure 2D) and with GO terms pathways associated to PPARα regulated pathways, such as “Cholesterol metabolic process” (*Acaa2*, *Apoa1)* and “Fatty acid beta-oxidation” (*Abcd3*, *Slc27a2*; Figure 2E). *Fat10* mRNA levels also correlate negatively with the expression of *Hmgcs2,* a PPARα target gene involved in ketogenesis (Figure 2F).

Altogether, these results demonstrate that FAT10 is induced specifically in hepatocytes in distinct murine models of MASH and correlates negatively with *Pparα* and its target genes suggesting a direct implication for FAT10 in the modulation of PPARα activity in hepatocytes.

4.3 FAT10 interacts with PPARα in human and mouse hepatocytes

Since interactions of FAT10 with other proteins modulate their expression or activity through a post-translational modification called FATylation [28], we next assessed whether FAT10 interacts with PPARα *in vitro* in hepatocytes overexpressing FAT10.

To mimic disease evolution to inflammatory MASH, PH were incubated with Tumor Necrosis Factor α (TNFα) and Interferon γ (IFNγ), two cytokines secreted in the liver during the transition from steatosis to MASH. Interestingly, *Fat10* gene expression was induced reaching a maximum after 24 h of cytokine treatment (Figure 3A). Similar inductions were observed both in HepG2 and immortalized human hepatocytes (IHH) at the gene (Suppl. Fig. 2A,B) and protein (Suppl. Fig. 2C,D) levels. Moreover, after 24 hours of cytokine treatment, FATylation activity was increased in HepG2 cells as shown by western blot analysis of the FATylated protein profile (Figure 3B). In these conditions, IF labelling revealed PPARα and FAT10 colocalization in the nucleus of HepG2 cells, suggesting a close proximity and hence, a possible direct interaction between these two proteins (Suppl. Fig. 2E).

Indeed, a direct interaction between FAT10 and PPARα in cytokine treated HepG2 and IHH cells was observed in a co-immunoprecipitation assay (Figure 3C). The FAT10-PPARα interaction was confirmed *in situ* by Proximity Ligation Assay (PLA), revealing an increased number of interactions not only in the nucleus, but also in the cytoplasm of cytokine treated HepG2 cells (Figure 3D). Finally, FAT10-PPARα interactions were observed by PLA also in murine MASH (CDAA) (Figure 3E) and human MASH patient livers (Figure 3F).

Altogether, these results demonstrate that FAT10 and PPARα interact *in vitro,* in hepatocytes upon FAT10 induction, and *in vivo,* in human and murine hepatocytes during MASH development.

4.4 FAT10 silencing enhances PPARα regulation of lipid metabolism in human hepatocytes

To analyse the functional impact of the FAT10-PPARα interaction on PPARα signaling, the effect of FAT10 siRNA knockdown (siFAT10) on PPARα activity was assessed in cytokine treated HepG2 cells (Suppl. Fig. 3A). Interestingly, knockdown of FAT10 increased PPARα target gene expression, whereas PPARα knockdown decreased mRNA levels of its target genes, such as *HMGCS2* and *PDK4*, measured by qPCR analysis (Figure 4A). In addition, PPARα downregulation, in combination with FAT10 knockdown, abrogated the increase in PPARα target gene expression demonstrating PPARα-dependency of the siFAT10 effect on PPARα target genes (Figure 4A).

Next, the impact of FAT10 downregulation on PPARα function was assessed by measuring lipid droplet accumulation and mitochondrial respiration in hepatocytes. PPARα downregulation increased, whereas FAT10 knockdown decreased the number of lipid droplets per cell as quantified by Bodipy staining (Figure 4B). However, the combined knockdown of FAT10 and PPARα reduced the effect of FAT10 knockdown on lipid droplet accumulation. Moreover, PPARα knockdown decreased, whereas FAT10 knockdown increased the maximal cellular respiration rate of the hepatocytes (Figure 4C). Again, combined FAT10 and PPARα knockdown decreased the effect of siFAT10 alone. These data demonstrate that FAT10 silencing increases mitochondrial activity and decreases lipid droplet accumulation by modulating PPARα activity.

Conversely, stable FAT10 overexpression in HepG2 cells after lentiviral infection (Suppl. Fig. 3B,C) increased lipid droplet accumulation (Suppl. Fig. 3D) and decreased the mitochondrial respiration rate (Suppl. Fig. 3E), both the basal and maximal oxygen consumption rate.

Altogether, these results demonstrate that FAT10 downregulation promotes PPARα activity and lipid metabolism in a PPARα-dependent manner, while FAT10 overexpression impairs lipid metabolism in human hepatocytes *in vitro*.

4.5 Hepatic FAT10 overexpression inhibits PPARα lipid metabolic activity in response to fasting *in vivo*

Next, the impact of ectopic FAT10 overexpression on the lipid metabolism regulatory activity of PPARα was investigated *in vivo*. Mice were first infected with adenoviruses targeting hepatocytes expressing either *Fat10* (Ad-FAT10) or not (Ad-CTRL). Since PPARα can be physiologically activated by fatty acids released from adipose tissue triglyceride lipolysis upon fasting, mice were subsequently either given free access to food, or submitted to an 18 hour fasting [29].

FAT10 expression was higher in livers of Ad-FAT10 compared to Ad-CTRL infected mice both at the protein (IF staining) and mRNA level (qPCR analysis) (Figure 5A). As expected, fasting slightly decreased the body weights in both groups of mice without changing the microscopic liver structure (Suppl. Fig. 4A,B) and increased *Pparα* mRNA levels in the livers of Ad-CTRL mice (Figure 5B). Interestingly, this induction was reduced in Ad-FAT10 mice and a negative correlation between hepatic *Fat10* and *Pparα* mRNA levels was observed under fasting conditions (Figure 5C).

In line, fasting increased the expression of several PPARα target genes, such as *Hmgcs2*, *Cpt1α* and *Aco,* in the livers of Ad-CTRL mice (Figure 5D). However, this induction was less pronounced in Ad-FAT10 mice and *Fat10* gene expression negatively correlated with the expression of several PPARα target genes (Figure 5E).

PLA analysis of livers of fasting Ad-CTRL and Ad-FAT10 mice revealed an enhanced interaction of FAT10 and PPARα both in the nucleus and cytoplasm of hepatocytes in Ad-FAT10 infected mice (Figure 5F).

These observations demonstrate that FAT10 overexpression *in vivo* leads to an interaction with PPARα and a decreased lipid gene regulatory activity of PPARα in response to fasting.

4.6 Hepatic FAT10 modulation impairs the PPARα agonist response to lipid metabolism *in vitro* and *in vivo*

Next, the impact of FAT10 knockdown and overexpression on PPARα activation by a synthetic agonist was investigated *in vitro* and *in vivo*. FAT10 knockdown in HepG2 cells (Suppl. Fig. 5A) significantly increased *HMGCS2* and *PDK4* mRNA levels (Figure 6A). Moreover, FAT10 knockdown enhanced the induction of these genes in response to pemafibrate indicating an increased metabolic response of PPARα to its agonist upon FAT10 downregulation.

Mice were then infected with Ad-FAT10 or Ad-CTRL and treated with pemafibrate (Suppl. Fig. 5B). To assess the specific impact of FAT10 overexpression on the response to pemafibrate, we first determined those genes significantly upregulated (p-value < 0.05 and FC (Fold Change) >1.5) by pemafibrate only in Ad-CTRL mice (“UP Pema”, Suppl. Fig. 6A,B). Then, the impact of FAT10 overexpression on the “UP Pema” genes was assessed (Figure 6B). Interestingly, FAT10 overexpression significantly dysregulated the lipid regulatory activities induced by pemafibrate

treatment. More specifically, the expression of genes related to “Metabolism of lipids”, “PPAR signaling pathway” and “Fatty acid metabolism” are decreased (Figure 6C). A closer look at the specific genes involved in these pathways shows that the expression of numerous pemafibrate-induced PPARα-target genes are decreased when FAT10 is overexpressed in mouse livers (Figure 6D).

These data indicate that FAT10 overexpression impairs PPARα signaling and inhibits its lipid regulatory activity in response to a synthetic agonist *in vitro* and *in vivo*.

4.7 Hepatic FAT10 overexpression inhibits the beneficial effect of PPARα agonist treatment on steatosis development *in vivo*

The impact of FAT10 overexpression on the lipid metabolic response to PPARα agonist treatment was studied *in vivo* in the CDAA mouse model of MASLD, which is characterized by a tremendous hepatic steatosis. After 2 weeks of CDAA diet, mice were infected with an adeno-associated virus (AAV) stably overexpressing *Fat10* specifically in hepatocytes (AAV-FAT10) or with a control AAV (AAV-CTRL), and the CDAA diet was continued for 3 more weeks. Finally, to induce PPARα activity, mice were treated with pemafibrate.

Immunohistochemical FAT10 staining of mouse livers showed that, as expected, FAT10 protein expression is increased by the CDAA diet in AAV-CTRL mice hepatocytes, and further enhanced in hepatocytes of AAV-FAT10 mice, validating the effectiveness of AAV infection (Figure 7A). Interestingly, the induction of PPARα-target genes, such as *Acadm*, *Ehhadh*, *Acox1* and *Cyp4a10* in response to pemafibrate was lower in mice overexpressing FAT10 (Figure 7B). Interestingly, the decrease in liver steatosis in response to pemafibrate treatment was lost in mice overexpressing FAT10

(Figure 7C). These results demonstrate that FAT10 induction hampers the improvement of MASLD-related liver steatosis by PPARα agonist treatment.

In summary, these data indicate that the induction of FAT10 in mouse hepatocytes during MASLD development inhibits ligand-induced PPARα activity against steatosis.

5. Discussion

The present study aimed at identifying mechanisms controlling PPARα activity during MASLD progression. Transcriptomic analysis of a large human cohort of patients allowed us to identify FAT10, a gene encoding an ubiquitin-like protein [17], as elevated in liver during MASLD progression. Similar findings showed FAT10 overexpression in livers of patients with chronic hepatic inflammation associated with MASH [24,30,31], alcoholic hepatitis [30] and HCC [32]. However, FAT10 is known to be constitutively expressed in immune cells, such as dendritic and Natural Killer T (NKT) cells, and its expression is induced by pro-inflammatory stimuli in B lymphocytes and monocytes [27]. These immune cells are known to infiltrate the liver during MASLD development, participating in disease progression [33] and could be responsible for the increase in FAT10 expression upon inflammation. Here, we demonstrate for the first time that *FAT10* is specifically induced in hepatocytes during MASLD progression. *FAT10* overexpression in hepatocytes is likely due to inflammation since data from us and others show that FAT10 expression is induced by pro-inflammatory cytokines such as TNFα/IFNγ acting via the NF-κB/STAT3 pathway [21], both in cancerous and non-cancerous hepatocytes *in vitro*. Interestingly, we observed a negative correlation between *Fat10* and *Pparα* expression in hepatocytes from murine and human MASLD livers. Since PPARα is predominantly expressed in hepatocytes, this result suggested that FAT10 induction in hepatocytes during MASLD progression may play a role in the dysfunction of PPARα signaling during disease development.

Indeed, we show that FAT10 downregulation reduces lipid content and promotes mitochondrial respiration. This improvement of lipid metabolism is associated with an increased expression of PPARα target genes such as *HMGCS2* and *PDK4*, in a

PPARα dependent manner. Interestingly, such target genes are regulated by PPARα through a transactivation mechanism [34] and previous data have shown that an increased expression of PPARα target genes, like *HMGCS2,* prevents steatosis development [35]. By contrast, FAT10 overexpression in mouse livers represses the induction of PPARα target gene expression in response to endogenous and exogenous PPARα ligands. Moreover, in a murine model of severe steatosis, the beneficial effects of PPARα activation by its agonist are lost when FAT10 is overexpressed in hepatocytes: FAT10 impairs lipid metabolism regulatory pathways and impairs the improvement of steatosis by PPARα agonist treatment. These results indicate that FAT10 acts on lipid metabolism by modulating PPARα activity in response to its ligands and, hence, is a modulator of PPARα-dependent lipid metabolism during MASLD progression.

FAT10 acts through an enzymatic cascade catalyzed by ligases resulting in its interaction with its partners [36]. This process, called FATylation, either promotes degradation [37,38] or stabilization [39,40] of its partners. Herein, we demonstrate that FAT10, upon cytokine induction, interacts with PPARα in hepatocytes identifying PPARα as a new FAT10 partner during MASH progression. Since PPARα is its own target gene acting through a PPARα response element in its own promoter [41], the post-translational modification of PPARα by FAT10 may partially explain the down-regulation of PPARα gene expression. Interestingly, FAT10 does not only induce degradation of its partners. For example, it has been shown to repress p53's transcriptional activity by changing its conformation [42] and to sequester the active form of RIG-I into insoluble protein aggregates [43]. Further experiments need to be done to test how exactly FAT10 modulates PPARα activity.

FAT10 interaction with PPARα also prevents its transcriptional induction by ligands whether they are natural or synthetic. Such observations could be part of the mechanisms explaining the disappointing results obtained in clinical studies with some PPARα specific or dual agonists. Indeed, fenofibrate [44] and elafibranor [45] displayed insufficient efficacy in resolving MASH parameters, especially steatosis in clinical studies. We propose that PPARα activity is repressed by FAT10, whose expression is induced in hepatocytes during MASLD, as such reducing agonist efficacy. Hence, inhibiting FAT10 or its binding to PPARα could be an approach to enhance PPARα activity and subsequently, the efficacy of its agonists in the treatment of MASLD. FAT10 can be indirectly targeted by a JAK2 inhibitor [46], but, unfortunately, this strategy lacks specificity. Inhibiting FATylation by targeting the ligases involved in FAT10 binding could also block FAT10's effect on PPARα activity. Such inhibitors have already been developed to inhibit NEDDylation by NEDD8, another ubiquitin-like post-translational modification. Under physiological conditions, NEDD8 is expressed and active in hepatocytes, but during the progression of liver fibrosis or the development of HCC, NEDDylation becomes aberrant and contributes to disease development [47,48]. NEDDylation inhibitor is now a promising therapy against liver cancer [49]. However, FAT10 has many partners [50] and targeting FAT10 or FATylation could impact all other proteins, inducing unwanted effects. Hence, strategies to specifically destabilize the FAT10-PPARα interaction is likely a better strategy.

5.1 Strengths and weaknesses of the study

A strength of this study is that our results are based on the analysis of human samples from a large cohort of patients with different MASLD stages and including both

transcriptomic and protein measurements. Also, our findings are validated in multiple models, notably *in vitro* in inflammatory hepatocytes and *in vivo* in mice in which FAT10 and PPARα expression could be modulated (knock-down and overexpression). Moreover, impaired lipid regulation activity of PPARα by FAT10 was demonstrated both upon physiological (fasting) and pharmacological (pemafibrate) activation of PPARα.

One of the limitations of this study is that the exact molecular mechanism of PPARα regulation by FAT10, which has a complex mode of action, required additional studies. Finally, further *in vivo* experiments on hepatocyte-specific FAT10 knockout mice are required to further study FAT10's effect on PPARα during experimental MASLD induction.

6. Conclusions

Overall, our study demonstrates that FAT10 expression is increased in hepatocytes by pro-inflammatory stimuli during progression of MASLD. The increase of FAT10 leads to an interaction with PPARα in human and murine hepatocytes. This interaction results in an impaired PPARα lipid regulatory activity in response to fasting or to PPARα agonists in physiological and pathological conditions. FAT10 acts as a negative modulator of PPARα lipid regulatory activity during MASLD development.

7. Acknowledgments

We thank M. Tardivel, A. Bongiovanni and S. Gabut of the BioImaging Center (Lille University School of Medicine Research centre) for expertise and training. We also thank the animal core facility of the Pasteur Institute Lille.

8. Author's contributions

Conceptualization: LC, LB, AKC, NH, CB, CD, AH, JTH, AV, CG, BD, EV, ED, LVG, GL, SF, BS, RP.

Investigation, Formal Analysis, Methodology: LC, LB, AKC, NH, CB, CD, AH, JTH, CG, BD, LG, JC, JE, EV, BS, RP.

Validation, Visualization: LC, LB, AKC, NH, CB, AH, JTH, AV, LVG, GL, SF, BS, RP.

Writing – original draft: LC, LB, BS, RP.

Writing – review & editing: LC, LB, BS, RP.

9. Funding information

This work was supported by: the Nouvelle Société Française d'Athérosclérose (NSFA, to LC), the FP7 "RESOLVE" (Grant ID: 305707 to BS, AV, SF, LVG) by FP6 "HEPADIP" (Contract LSHM-CT-2005-018734 to SF, LVG, BS), the European Genomic Institute for Diabetes (EGID, ANR-10-LABX-0046 to BS), the Agence Nationale de la Recherche PreciNASH (ANR-16-RHUS-0006 to BS), DeCodeNASH (ANR-20-CE14-0034 to JTH), the Fondation pour la Recherche Médicale (EQU202203014650), the Association Française pour l'Etude du Foie (AFEF, to RP), the Contrat Plan État-Région Hauts-de-France-Centre Transdisciplinaire de la Recherche sur la Longévité (CPER-CTRL) (to RP, AC and LB), an ERC Starting Grant (Metabo3DC no.101042759) (to JTH) and France Relance (ANR-21-PRRD-0076-01 to RP, BS, CB and CD). LC was supported by a PhD fellowship from Institut Pasteur de Lille and Région Haut de France (France). LB was supported by a PhD fellowship from Centre Hospitalier Universitaire (CHU) de Lille and by the "Health PhD 2020" scolarship of I-Site Université de Lille Nord Europe (ULNE) (France). JTH was supported by an EMBO Long Term Fellowship (ALTF 277-2014). SF received a senior clinical research fellowship from the Research Foundation Flanders (1802154N). The project was also partially funded by the Antwerp University (GOA 2018, ID36572).

10. Declarations of interest

None.

11. References

[1] Rinella ME, Lazarus J V., Ratziu V, Francque SM, Sanyal AJ, Kanwal F, et al. A multi-society Delphi consensus statement on new fatty liver disease nomenclature. J Hepatol 2023. https://doi.org/10.1016/j.jhep.2023.06.003.

[2] Mitra S, De A, Chowdhury A. Epidemiology of non-alcoholic and alcoholic fatty liver diseases. Translational Gastroenterology and Hepatology 2020;5:1–17. https://doi.org/10.21037/TGH.2019.09.08.

[3] Haas JT, Francque S, Staels B. Pathophysiology and Mechanisms of Nonalcoholic Fatty Liver Disease. Annual Review of Physiology 2016. https://doi.org/10.1146/annurev-physiol-021115-105331.

[4] Montaigne D, Butruille L, Staels B. PPAR control of metabolism and cardiovascular functions. Nature Reviews Cardiology 2021;18:809–23. https://doi.org/10.1038/s41569-021-00569-6.

[5] Younossi Z, Anstee QM, Marietti M, Hardy T, Henry L, Eslam M, et al. Global burden of NAFLD and NASH: Trends, predictions, risk factors and prevention. Nature Reviews Gastroenterology and Hepatology 2018;15:11–20. https://doi.org/10.1038/nrgastro.2017.109.

[6] **Ferguson D, Finck BN**. Emerging therapeutic approaches for the treatment of NAFLD and type 2 diabetes mellitus. Nature Reviews Endocrinology 2021;17:484–95. https://doi.org/10.1038/s41574-021-00507-z.

[7] Pawlak M, Lefebvre P, Staels B. Molecular mechanism of PPARα action and its impact on lipid metabolism, inflammation and fibrosis in non-alcoholic fatty liver disease. Journal of Hepatology 2015;62:720–33. https://doi.org/10.1016/j.jhep.2014.10.039.

[8] Montagner A, Polizzi A, Fouché E, Ducheix S, Lippi Y, Lasserre F, et al. Liver PPARα is crucial for whole-body fatty acid homeostasis and is protective against NAFLD. Gut 2016;65:1202–14. https://doi.org/10.1136/gutjnl-2015-310798.

[9] Lalloyer F, Wouters K, Baron M, Caron S, Vallez E, Vanhoutte J, et al. Peroxisome proliferator-activated receptor-α gene level differently affects lipid metabolism and inflammation in apolipoprotein E2 knock-in mice. Arteriosclerosis, Thrombosis, and Vascular Biology 2011;31:1573–9. https://doi.org/10.1161/ATVBAHA.110.220525.

[10] Ip E, Farrell G, Hall P, Robertson G, Leclercq I. Administration of the Potent PPARα Agonist, Wy-14,643, Reverses Nutritional Fibrosis and Steatohepatitis in Mice. Hepatology 2004;39:1286–96. https://doi.org/10.1002/hep.20170.

[11] **Shiri-Sverdlov R, Wouters K**, Gorp PJV, Gijbels MJ, Noel B, Buffat L, et al. Early diet-induced non-alcoholic steatohepatitis in APOE2 knock-in mice and its prevention by fibrates. Journal of Hepatology 2006;44:732–41. https://doi.org/10.1016/j.jhep.2005.10.033.

[12] Hennuyer N, Duplan I, Paquet C, Vanhoutte J, Woitrain E, Touche V, et al. The novel selective PPARα modulator (SPPARMα) pemafibrate improves dyslipidemia, enhances reverse cholesterol transport and decreases inflammation and atherosclerosis. Atherosclerosis 2016;249:200–8. https://doi.org/10.1016/j.atherosclerosis.2016.03.003.

[13] Pawlak M, Baugé E, Bourguet W, De Bosscher K, Lalloyer F, Tailleux A, et al. The transrepressive activity of peroxisome proliferator-activated receptor alpha is necessary and sufficient to prevent liver fibrosis in mice. Hepatology 2014;60:1593–606. https://doi.org/10.1002/hep.27297.

[14] **Francque S, Verrijken A**, Caron S, Prawitt J, Paumelle R, Derudas B, et al. PPARa gene expression correlates with severity and histological treatment response in patients with Non-alcoholic Steatohepatitis. JOURNAL OF HEPATOLOGY 2015. https://doi.org/10.1016/j.jhep.2015.02.019.

[15] Okishio S, Yamaguchi K, Ishiba H, Tochiki N, Yano K, Takahashi A, et al. PPARα agonist and metformin co-treatment ameliorates NASH in mice induced by a choline-deficient, amino acid-defined diet with 45% fat. Scientific Reports 2020;10:1–11. https://doi.org/10.1038/s41598-020-75805-z.

[16] Ratziu V, Harrison SA, Francque S, Bedossa P, Lehert P, Serfaty L, et al. Elafibranor, an Agonist of the Peroxisome Proliferator-Activated Receptor-α and -δ, Induces Resolution of Nonalcoholic Steatohepatitis Without Fibrosis Worsening. Gastroenterology 2016;150:1147-1159e5. https://doi.org/10.1053/j.gastro.2016.01.038.

[17] Fan W, Cai W, Parimoo S, Lennon GG, Weissman SM. Identification of seven new human MHC class I region genes around the HLA-F locus. Immunogenetics 1996;44:97–103. https://doi.org/10.1007/BF02660056.

[18] Aichem A, Anders S, Catone N, Rößler P, Stotz S, Berg A, et al. The structure of the ubiquitin-like modifier FAT10 reveals an alternative targeting mechanism for proteasomal degradation. Nature Communications 2018;9:1–14. https://doi.org/10.1038/s41467-018-05776-3.

[19] Schmidtke G, Aichem A, Groettrup M. FAT10ylation as a signal for proteasomal degradation. Biochimica et Biophysica Acta - Molecular Cell Research 2014. https://doi.org/10.1016/j.bbamcr.2013.01.009.

[20] **Kalveram B, Schmidtke G, Groettrup M**. The ubiquitin-like modifier FAT10 interacts with HDAC6 and localizes to aggresomes under

proteasome inhibition. Journal of Cell Science 2008. https://doi.org/10.1242/jcs.035006.

[21] Choi Y, Kim JK, Yoo JY. NFκB and STAT3 synergistically activate the expression of FAT10, a gene counteracting the tumor suppressor p53. Molecular Oncology 2014. https://doi.org/10.1016/j.molonc.2014.01.007.

[22] **Bantubungi K, Hannou SA**, Caron-Houde S, Vallez E, Baron M, Lucas A, et al. Cdkn2a/p16Ink4aregulates fasting-induced hepatic gluconeogenesis through the PKA-CREB-PGC1 α pathway. Diabetes 2014;63:3199–209. https://doi.org/10.2337/db13-1921.

[23] Haas JT, Vonghia L, Mogilenko DA, Verrijken A, Molendi-Coste O, Fleury S, et al. Transcriptional network analysis implicates altered hepatic immune function in NASH development and resolution. Nature Metabolism 2019;1:604–14. https://doi.org/10.1038/s42255-019-0076-1.

[24] Dali-Youcef N, Vix M, Costantino F, El-Saghire H, Lhermitte B, Callari C, et al. Interleukin-32 Contributes to Human Nonalcoholic Fatty Liver Disease and Insulin Resistance. Hepatology CommuniCations 2019;3:1205–20. https://doi.org/10.1002/hep4.1396/suppinfo.

[25] Kleiner DE, Brunt EM, Van Natta M, Behling C, Contos MJ, Cummings OW, et al. Design and validation of a histological scoring system for nonalcoholic fatty liver disease. Hepatology 2005;41:1313–21. https://doi.org/10.1002/hep.20701.

[26] **Kita Y, Takamura T**, Misu H, Ota T, Kurita S, Takeshita Y, et al. Metformin Prevents and Reverses Inflammation in a Non-Diabetic Mouse Model of Nonalcoholic Steatohepatitis. PLoS ONE 2012;7. https://doi.org/10.1371/journal.pone.0043056.

[27] Schregle R, Mah MM, Mueller S, Aichem A, Basler M, Groettrup M. The expression profile of the ubiquitin-like modifier FAT10 in immune cells suggests cell type-specific functions. Immunogenetics 2018;70:429–38. https://doi.org/10.1007/s00251-018-1055-5.

[28] Aichem A, Groettrup M. The ubiquitin-like modifier FAT10 - much more than a proteasome-targeting signal. Journal of Cell Science 2020;133. https://doi.org/10.1242/jcs.246041.

[29] Kersten S, Seydoux J, Peters JM, Gonzalez FJ, Desvergne B, Wahli W. Peroxisome proliferator-activated receptor α mediates the adaptive response to fasting. Journal of Clinical Investigation 1999;103:1489–98. https://doi.org/10.1172/JCI6223.

[30] Jia Y, French B, Tillman B, French S. Different roles of FAT10, FOXO1, and ADRA2A in hepatocellular carcinoma tumorigenesis in patients with alcoholic steatohepatitis (ASH) vs non-alcoholic steatohepatitis (NASH). Experimental and Molecular Pathology 2018. https://doi.org/10.1016/j.yexmp.2018.07.005.

[31] Vandel J, Dubois-Chevalier J, Gheeraert C, Derudas B, Raverdy V, Thuillier D, et al. Hepatic molecular signatures highlight the sexual dimorphism of Non-Alcoholic SteatoHepatitis (NASH). Hepatology 2020. https://doi.org/10.1002/hep.31312.

[32] **Zhang Y, Zuo Z, Liu B**, Yang P, Wu J, Han L, et al. FAT10 promotes hepatocellular carcinoma (HCC) carcinogenesis by mediating P53 degradation and acts as a prognostic indicator of HCC. Journal of Gastrointestinal Oncology 2021;12:1823–37. https://doi.org/10.21037/jgo-21-374.

[33] Cai J, Zhang XJ, Li H. The Role of Innate Immune Cells in Nonalcoholic Steatohepatitis. Hepatology 2019;70:1026–37. https://doi.org/10.1002/hep.30506.

[34] Rakhshandehroo M, Knoch B, Michael M, Kersten S. Peroxisome Proliferator-Activated Receptor Alpha Target Genes 2010;2010. https://doi.org/10.1155/2010/612089.

[35] **Asif S, Kim RY**, Fatica T, Sim J, Zhao X, Oh Y, et al. Hmgcs2-mediated ketogenesis modulates high-fat diet-induced hepatosteatosis. Molecular Metabolism 2022;61:101494. https://doi.org/10.1016/j.molmet.2022.101494.

[36] Aichem A, Pelzer C, Lukasiak S, Kalveram B, Sheppard PW, Rani N, et al. USE1 is a bispecific conjugating enzyme for ubiquitin and FAT10, which FAT10ylates itself in cis. Nature Communications 2010;1. https://doi.org/10.1038/ncomms1012.

[37] Aichem A, Kalveram B, Spinnenhirn V, Kluge K, Catone N, Johansen T, et al. The proteomic analysis of endogenous FAT10 substrates identifies p62 / SQSTM1 as a substrate of FAT10ylation. Journal of Cell Science 2012;53:4576–85. https://doi.org/10.1242/jcs.107789.

[38] Chen Z, Zhang WEI, Yun Z, Zhang XUE, Gong F, Wang Y, et al. Ubiquitin - like protein FAT10 regulates DNA damage repair via modification of proliferating cell nuclear antigen. Molecular Medicine Reports 2018:7487–96. https://doi.org/10.3892/mmr.2018.8843.

[39] **Yuan R, Wang K**, Hu J, Yan C, Li M, Yu X, et al. Ubiquitin-like Protein FAT10 Promotes the Invasion and Metastasis of Hepatocellular Carcinoma by Modifying b -Catenin Degradation. Cancer Res 2014. https://doi.org/10.1158/0008-5472.CAN-14-0284.

[40] **Liu X, Chen L, Ge J**, Yan C, Huang Z, Hu J, et al. The Ubiquitin-like Protein FAT10 Stabilizes eEF1A1 Expression to Promote Tumor Proliferation in a Complex Manner. Cancer Res 2016:4897–908. https://doi.org/10.1158/0008-5472.CAN-15-3118.

[41] Pineda-Torra I, Jamshidi Y, Flavell DM, Fruchart J-C, Staels B. Characterization of the Human PPAR alpha Promoter : Identification of a

Functional Nuclear Response Element. Molecular Endocrinology 2002;16:1013–28.

[42] Li T, Santockyte R, Yu S, Shen R-F, Tekle E, Lee CG, et al. FAT10 modifies p53 and upregulates its transcriptional activity. Arch Biochem Biophys 2011. https://doi.org/10.1016/j.abb.2011.02.017.FAT10.

[43] **Nguyen NTH, Now H**, Kim WJ, Kim N, Yoo JY. Ubiquitin-like modifier FAT10 attenuates RIG-I mediated antiviral signaling by segregating activated RIG-I from its signaling platform. Scientific Reports 2016;6:1–12. https://doi.org/10.1038/srep23377.

[44] Oscarsson J, Önnerhag K, Risérus U, Sundén M, Johansson L, Jansson PA, et al. Effects of free omega-3 carboxylic acids and fenofibrate on liver fat content in patients with hypertriglyceridemia and non-alcoholic fatty liver disease: A double-blind, randomized, placebo-controlled study. Journal of Clinical Lipidology 2018;12:1390-1403.e4. https://doi.org/10.1016/j.jacl.2018.08.003.

[45] Ratziu V, Harrison SA, Francque S, Bedossa P, Lehert P, Serfaty L, et al. Elafibranor, an Agonist of the Peroxisome Proliferator-Activated Receptor-α and -δ, Induces Resolution of Nonalcoholic Steatohepatitis Without Fibrosis Worsening. Gastroenterology 2016;150:1147-1159.e5. https://doi.org/10.1053/j.gastro.2016.01.038.

[46] Reznik N, Kozer N, Eisenberg-Lerner A, Barr H, Merbl Y, London N. Phenotypic Screen Identifies JAK2 as a Major Regulator of FAT10 Expression. ACS Chemical Biology 2019;14:2538–45. https://doi.org/10.1021/acschembio.9b00667.

[47] **Yu J, Huang W long**, Xu Q guo, Zhang L, Sun S han, Zhou W ping, et al. Overactivated neddylation pathway in human hepatocellular carcinoma. Cancer Medicine 2018;7:3363–72. https://doi.org/10.1002/cam4.1578.

[48] Zubiete-Franco I, Fernández-Tussy P, Barbier-Torres L, Simon J, Fernández-Ramos D, Lopitz-Otsoa F, et al. Deregulated neddylation in liver fibrosis. Hepatology 2017;65:694–709. https://doi.org/10.1002/hep.28933.

[49] Yang Z, Zhang J, Lin X, Wu D, Li G, Zhong C, et al. Inhibition of neddylation modification by MLN4924 sensitizes hepatocellular carcinoma cells to sorafenib. Oncology Reports 2019;41:3257–69. https://doi.org/10.3892/or.2019.7098.

[50] Leng L, Xu C, Wei C, Zhang J, Liu B, Ma J, et al. A proteomics strategy for the identification of FAT10-modified sites by mass spectrometry. Journal of Proteome Research 2014;13:268–76. https://doi.org/10.1021/pr400395k.

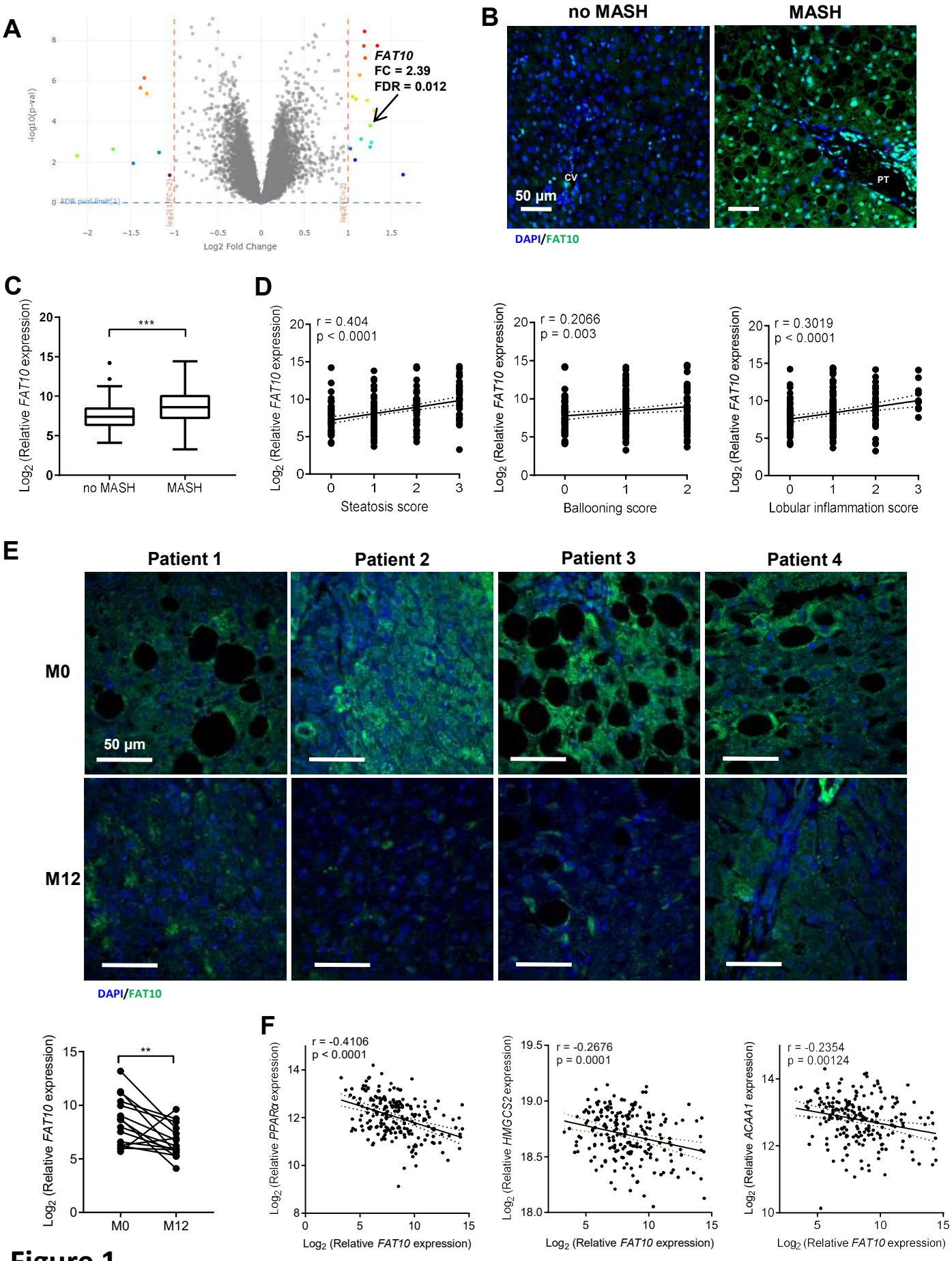
A
FAT10
FC = 2.39
FDR = 0.012
-log10(p-val)
Log2 Fold Change
B
no MASH
MASH
CV
PT
50 µm
DAPI/FAT10
C
Log2 (Relative FAT10 expression)
***
no MASH
MASH
D
r = 0.404
p < 0.0001
Steatosis score
r = 0.2066
p = 0.003
Ballooning score
r = 0.3019
p < 0.0001
Lobular inflammation score
E
Patient 1
Patient 2
Patient 3
Patient 4
M0
M12
50 µm
DAPI/FAT10
**
M0
M12
F
r = -0.4106
p < 0.0001
Log2 (Relative PPARα expression)
r = -0.2676
p = 0.0001
Log2 (Relative HMGCS2 expression)
r = -0.2354
p = 0.00124
Log2 (Relative ACAA1 expression)
Log2 (Relative FAT10 expression)

Figure 1

Figure 1: FAT10 is elevated in MASH patient livers and correlates negatively with *PPARα* expression.

Livers from 205 patients were sorted according to histological score (steatosis (S), inflammation (I), fibrosis (F) and ballooning (B)) used to calculate the Non alcoholic fatty liver disease Activity Score (NAS) (S + I + B) into « no MASH » (MASH: Metabolic-dysfunction Steatohepatitis) (NAS ≤ 3 without S ≥ 1 + B ≥ 1 + I ≥ 1) (N = 77) or « MASH » (NAS ≥ 3 with S ≥ 1 + B ≥ 1 + I ≥ 1) (N = 128) and transcriptomic analyzes were performed. A) Volcano plots of average log2 fold-changes versus p-values of all patients' transcripts. The fold change (FC) and false discovery rate (FDR) for the human leukocyte antigen-F Adjacent Transcript 10 (FAT10) are indicated. B) Representative images for the immunostaining of liver sections from no MASH (S < 33 %, I = 0, B = 0 and F = 0) or MASH (S > 5 %, I > 1, B = 2 and F < 3) patients. Nuclear staining in blue with DAPI and FAT10 staining in green enhanced by tyramide detection. The central vein (CV) and portal triad (PT) are indicated. Scale bar: 50 µm. C) *FAT10* gene expression was measured in livers of patients with versus without histologically diagnosed MASH (data are represented as box and whiskers in Tukey style, p-value for no MASH vs MASH ** p < 0.01). D) Correlation between *FAT10* gene expression and each histological grade of Metabolic-dysfunction Associated Steatotic Liver Disease (MASLD). E) Representative images for the immunostaining of liver sections from patients before (M0, with S > 5 %, I > 1, B = 2 and F < 3) and 12 months after a weight loss thanks to a bariatric surgery (M12, S < 33 %, I = 0, B = 0 and F = 0) for 4 representative patients. Nuclear staining in blue with DAPI, FAT10 staining in green enhanced by tyramide detection. Scale bar: 50 µm. A graph showing *FAT10* relative mRNA expression at M0 and M12 for all patients (N=15) is associated (p-value for M0 vs M12 ** p < 0.01). F) Correlation between *FAT10* and the Peroxisome Proliferator-Activated Receptor α (*PPARα*) gene expression or some of its target genes 3-hydroxy-3-methylglutaryl-CoA synthase 2 (*HMGCS2*) and Acetyl-CoA Acyltransferase 1 (*ACAA1*). The correlations are linear regressions, the p-values, p, and the correlation coefficient, r, are indicated. The best fit curve is shown with a line and the 95% confidence bands are represented with a dashed line.

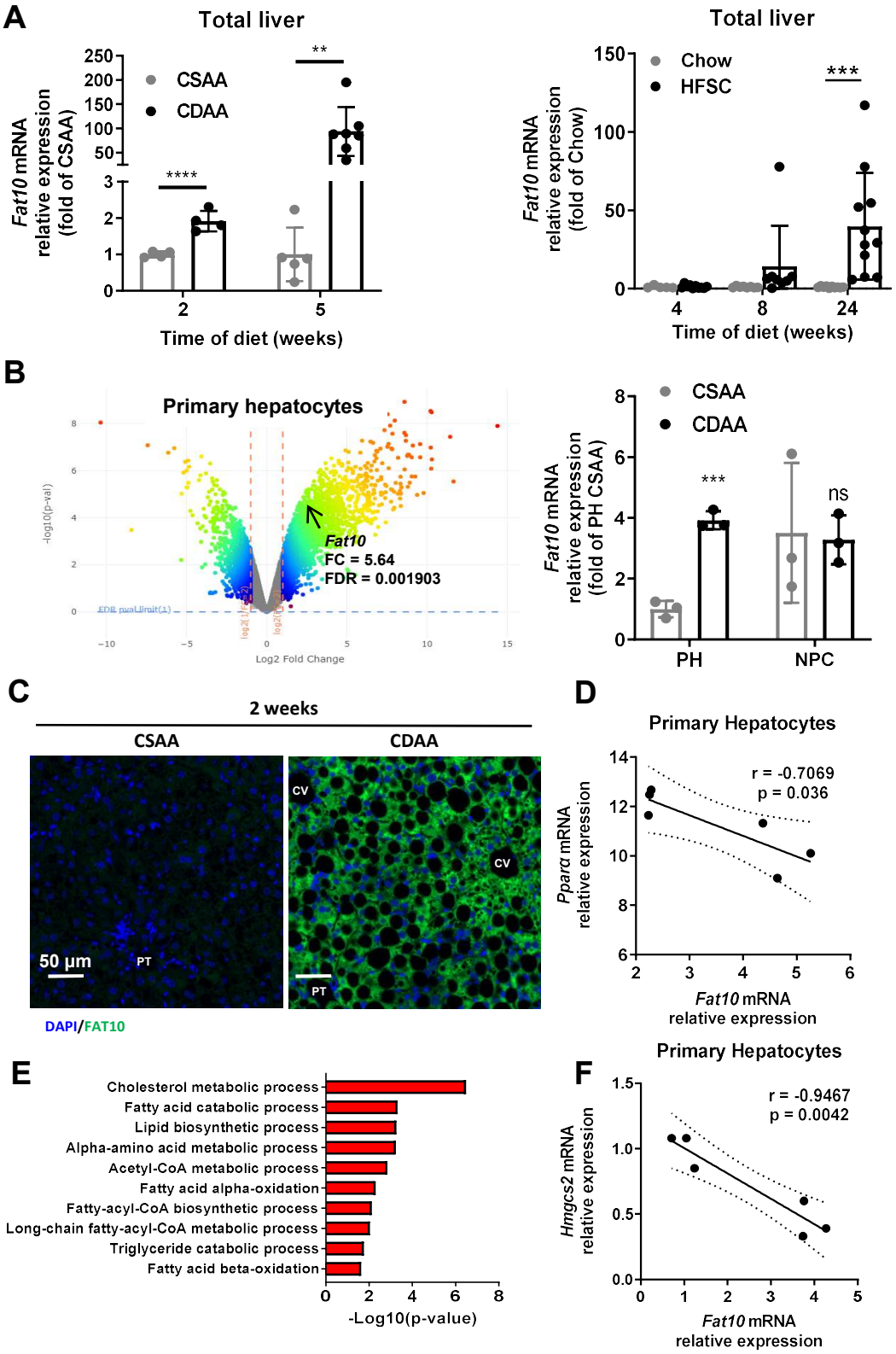
A
Total liver
Fat10 mRNA relative expression (fold of CSAA)
CSAA
CDAA
****
**
Time of diet (weeks)
Total liver
Fat10 mRNA relative expression (fold of Chow)
Chow
HFSC
***
Time of diet (weeks)
B
Primary hepatocytes
Fat10
FC = 5.64
FDR = 0.001903
Log2 Fold Change
Fat10 mRNA relative expression (fold of PH CSAA)
CSAA
CDAA
***
ns
PH
NPC
C
2 weeks
CSAA
CDAA
CV
50 µm
PT
DAPI/FAT10
D
Primary Hepatocytes
r = -0.7069
p = 0.036
Pparα mRNA relative expression
Fat10 mRNA relative expression
E
Cholesterol metabolic process
Fatty acid catabolic process
Lipid biosynthetic process
Alpha-amino acid metabolic process
Acetyl-CoA metabolic process
Fatty acid alpha-oxidation
Fatty-acyl-CoA biosynthetic process
Long-chain fatty-acyl-CoA metabolic process
Triglyceride catabolic process
Fatty acid beta-oxidation
-Log10(p-value)
F
Primary Hepatocytes
r = -0.9467
p = 0.0042
Hmgcs2 mRNA relative expression
Fat10 mRNA relative expression

Figure 2

Figure 2: FAT10 is overexpressed in hepatocytes and correlates negatively with Pparα during MASH development in murine livers.

Male mice were fed with a choline deficient diet enriched with 1 % cholesterol, glucose and fructose (CDAA) or a control diet (CSAA) during 2 weeks (CSAA N = 4 and CDAA N = 4) or 5 weeks (CSAA N = 5 and CDAA N = 7) and total livers or primary hepatocytes (PH) and non-parenchymal cells (NPC) (CSAA N = 3 and CDAA N = 3, only for 2 weeks) were collected. A) The human leukocyte antigen-F adjacent transcript 10 *(Fat10)* gene expression in total livers of mice after 2 and 5 weeks of diet measured by qPCR, and *Fat10* gene expression on mice total livers from male mice fed with a high fat diet supplemented with sucrose and cholesterol (HFSC) or a Chow diet during 4 (Chow N = 5 and HFSC N = 10), 8 (Chow N = 8 and HFSC N = 8), and 24 weeks (Chow N = 10 and HFSC N = 11). B) Volcano plot of PH from CSAA vs CDAA mice after 2 weeks of diet, and *Fat10* gene expression in PH or NPC of CSAA and CDAA mice after 2 weeks of diet measured by qPCR. C) Representative images for the immunofluorescence of the livers of mice after 2 weeks of CSAA or CDAA. Nuclear staining in blue with DAPI and FAT10 protein staining in green enhanced by tyramide detection. The central veins (CV) and portal triads (PT) are indicated. Scale bar: 50 µm. D) Correlation between *Fat10* and the Peroxisome proliferator-activated receptor α (*Pparα*) expression in the PH isolated from mice under 2 weeks of diet obtained from transcriptomic data. The correlation is a linear regression, the p-value and correlation coefficient r are indicated. The best fit curve is shown with a line and the 95% confidence bands are represented with a dashed line. E) Gene ontology terms enrichment for genes that are negatively correlated to *Fat10* expression in primary hepatocytes isolated from mice under 2 weeks of diet obtained from transcriptomic data. F) Correlation between *Fat10* and 3-Hydroxy-3-methylglutaryl-CoA synthase 2 (*Hmgcs2*) gene expression in the PH isolated from mice under 2 weeks of diet obtained from transcriptomic data. The correlation is a linear regression, the p-value and correlation coefficient r are indicated. The best fit curve is shown with a line and the 95% confidence bands are represented with a dashed line.

Mean values are indicated ± SEM and with unpaired t-test or two-way ANOVA (**** $p < 0.0001$, *** $p < 0.001$ and ** $p < 0.01$).

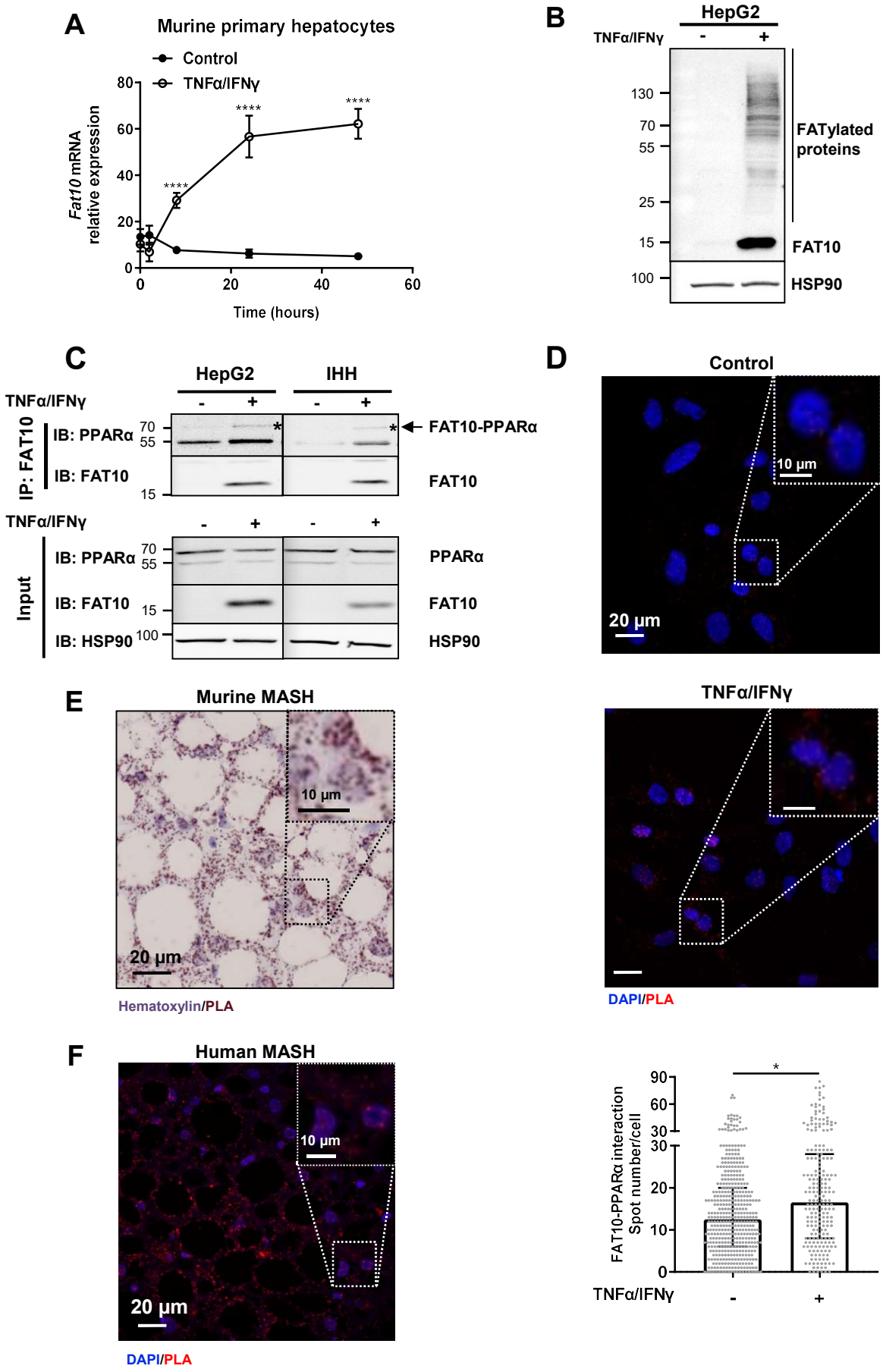
A
Murine primary hepatocytes
Control
TNFα/IFNγ
Fat10 mRNA relative expression
Time (hours)
****
B
HepG2
TNFα/IFNγ
FATylated proteins
FAT10
HSP90
C
HepG2
IHH
TNFα/IFNγ
IP: FAT10
IB: PPARα
IB: FAT10
FAT10-PPARα
Input
IB: HSP90
PPARα
D
Control
10 μm
20 μm
E
Murine MASH
Hematoxylin/PLA
TNFα/IFNγ
DAPI/PLA
F
Human MASH
DAPI/PLA
FAT10-PPARα interaction Spot number/cell
*

Figure 3

Figure 3: FAT10 interacts with PPARα in human and murine hepatocytes.
A) The human leukocyte antigen-F adjacent transcript 10 (*Fat10*) mRNA gene expression measured by qPCR in murine primary hepatocytes treated with murine Tumor Necrosis Factor α (TNFα) (50 ng/mL) and Interferon γ (IFNγ) (10 ng/mL) (TNFα/IFNγ) or with sterile water (control) during 8 h, 24 h or 48 h. Values are mean ± SD analyzed by two-way ANOVA (**** $p<0.0001$). B) Western blot of free FAT10 and FATylated proteins in HepG2 cells treated with human TNFα (50 ng/mL) and IFNγ (10 ng/mL) (TNFα/IFNγ) or not during 24 h. C) HepG2 cells and Immortalized Human Hepatocytes (IHH) cells were treated with TNFα/IFNγ during 24 h as described before. Cell lysates were subjected to immunoprecipitation with anti-FAT10 antibody. Western blot analysis was performed with antibodies reactive against the Peroxisome Proliferator-Activated Receptor α (PPARα) or FAT10. Heat Shock Protein 90 (HSP90) was used as a loading control. Upper panels show the immunoprecipitated proteins and lower panels show the total protein expression in the cell lysates (Input). The asterisks mark bands corresponding to the FAT10-PPARα complexes. IB: Immunoblotting, IP: Immunoprecipitation. Representative images for the Proximity Ligation Assay (PLA) targeting FAT10 and PPARα performed on D) HepG2 cells treated or not with TNFα/IFNγ during 24 h and quantified with Image J represented as median with interquartile range analyzed by unpaired t-test (* $p < 0.05$), E) liver sections from mice fed with choline deficient diet enriched with 1 % cholesterol, glucose and fructose (CDAA) during 2 weeks and F) liver sections from Metabolic-dysfunction Associated Steatohepatitis (MASH) (steatosis > 5%, inflammation > 1, ballooning = 2 and fibrosis < 3) patients from the cohort. Images are represented full (scale bar: 20 µm) with a zoom on a selected representative zone (scale bar: 10 µm). Nuclear staining in blue with hematoxylin and PLA detection in red.

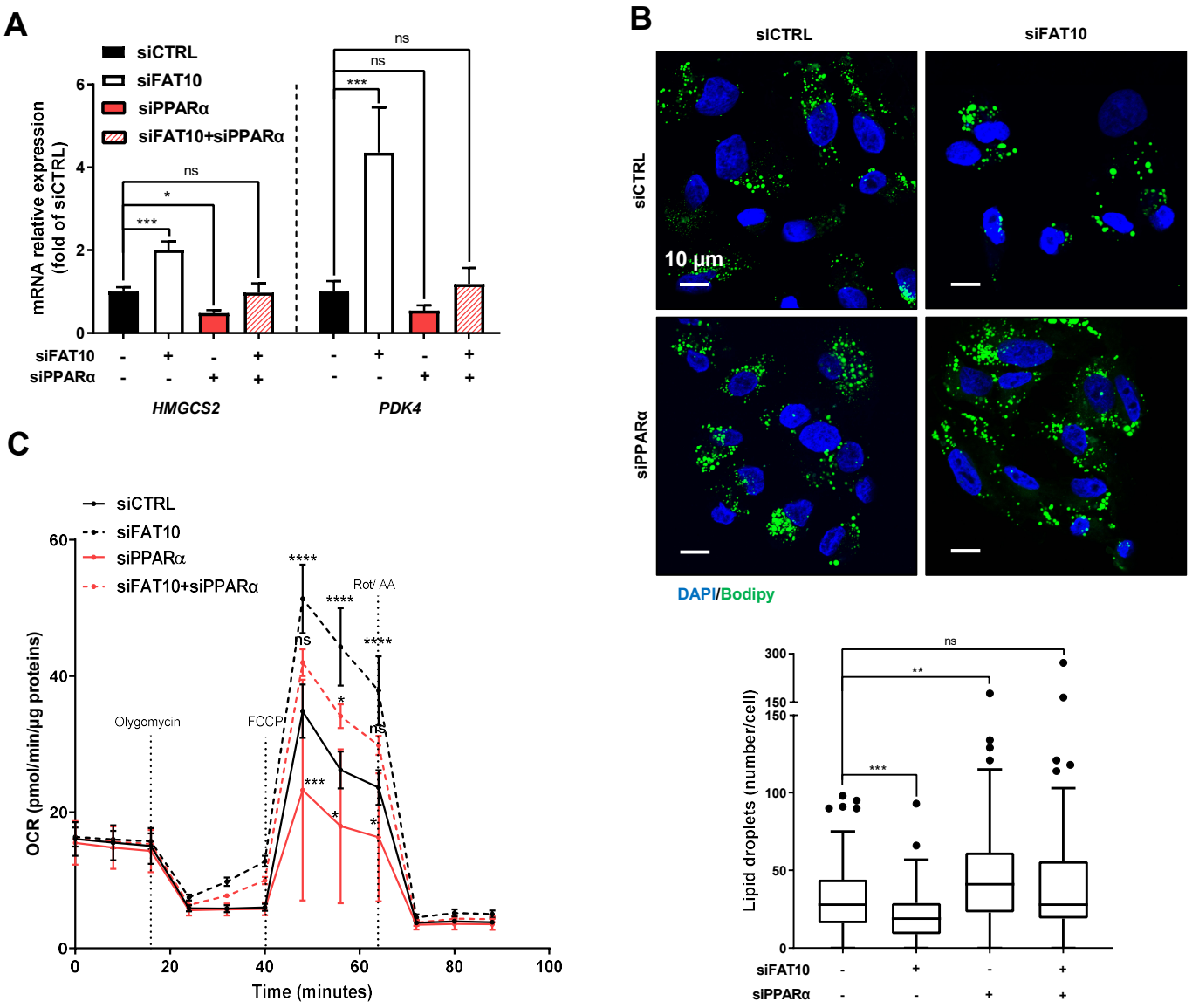
A
siCTRL
siFAT10
siPPARα
siFAT10+siPPARα
mRNA relative expression (fold of siCTRL)
ns
***
*
siFAT10
siPPARα
HMGCS2
PDK4
B
siCTRL
siFAT10
siCTRL
siPPARα
10 µm
DAPI/Bodipy
Lipid droplets (number/cell)
C
OCR (pmol/min/µg proteins)
Olygomycin
FCCP
Rot/ AA
Time (minutes)

Figure 4

Figure 4: FAT10 silencing enhances PPARα regulation of lipid metabolism in human hepatocytes. HepG2 cells were transfected with a siRNA control (siCTRL) or a siRNA targeting the human leukocyte antigen-F Adjacent Transcript 10 (FAT10) (siFAT10) with or without a siRNA targeting the Peroxisome Proliferator-Activated Receptor α (PPARα) (siPPARα) during 24 h and then treated with human Tumor Necrosis Factor α (TNFα) (50 ng/mL) and Interferon γ (IFNγ) (10 ng/mL) (TNFα/IFNγ) during 24 h. A) 3-hydroxy-3-methylglutaryl-CoA synthase (*HMGCS2*) 2) and Pyruvate Dehydrogenase 4 (*PDK4*) mRNA gene expression measured by qPCR. B) Representative images of BODIPY 493/503 staining of neutral lipids (scale bar: 20 µm) with the quantification of lipid droplets per cell using the spot detection plug-in of the Icy software. C) Oxygen Consumption Rate (OCR) in HepG2 cells transfected with either siCTRL or siFAT10 with or without siPPARα for 48 h, and incubated for 1 h in Seahorse assay media complemented with 1 mM pyruvate, 200 mM glutamine and 10 mM glucose. OCR was measured over time after treatment with Oligomycin (2 µM), ATP synthase inhibitor; FCCP (1 µM), mitochondrial uncoupler; and rotenone and antimycin A (Rot/AA) (0.5 µM), specific inhibitors for ETC complex I and III, respectively. Values are mean ± SD analyzed by two-way ANOVA (siCTRL vs siRNA **** $p < 0.0001$, *** $p < 0.001$, ** $p < 0.01$, * $p < 0.05$, ns $p > 0.05$).

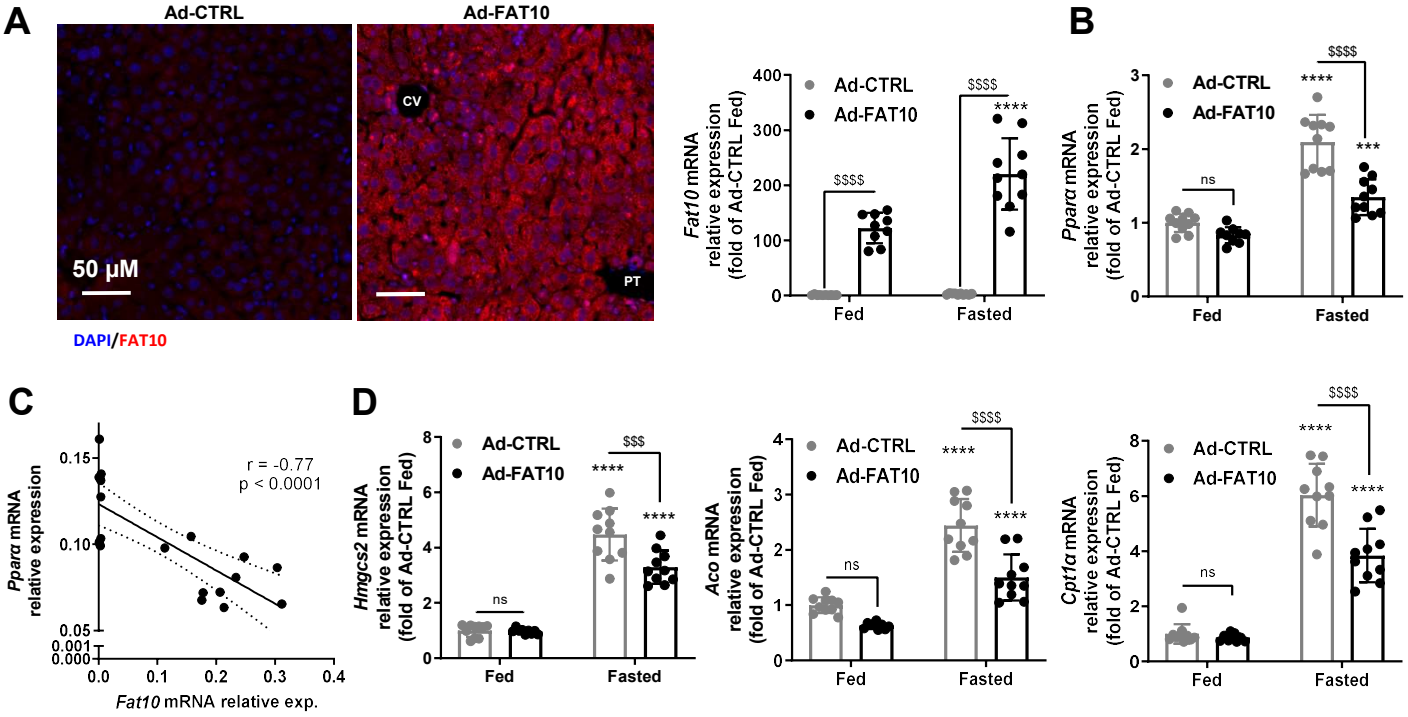

E

	Gene symbol	Correlation with *Fat10* mRNA level (r)	Correlation with *Fat10* mRNA level (p-value)
	Pparα	-0.77	< 0.0001
Ketogenesis	*Hmgcs2*	-0.66	0.0017
Mitochondrial FAO	*Cpt1α*	-0.77	< 0.0001
	Acadvl	-0.45	0.0452
	Acadl	-0.55	0.0112
	Acadm	-0.55	0.0127
Peroxysomal FAO	*Aco*	-0.80	< 0.0001
Microsomal FAO	*Cyp4a10*	-0.85	< 0.0001
TG desaturation	*Scd1*	-0.75	0.0001

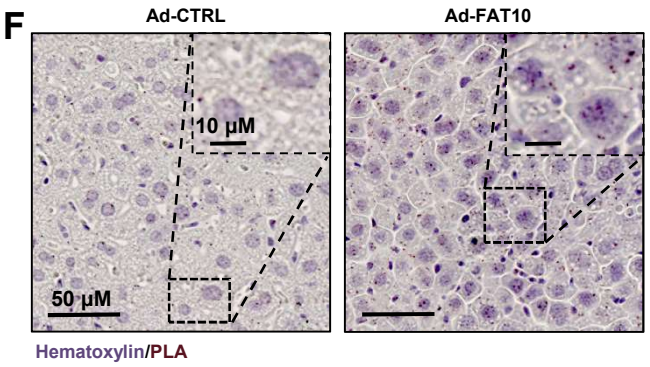

Figure 5

Figure 5: Hepatic FAT10 overexpression inhibits PPARα lipid metabolic activity in response to fasting in vivo.

8 week–old male mice were injected with a control adenovirus (Ad-CTRL) (N = 20) or adenovirus overexpressing the human leukocyte antigen-F Adjacent Transcript 10 (FAT10) (Ad-FAT10) (N = 19) during 4 days. Then mice were fed *ad libitum* (Ad-CTRL fed N = 10, Ad-FAT10 fed N = 9) or fasted during 18h (Ad-CTRL fasted N = 10, Ad-FAT10 fasted N = 10) before livers were collected. A) Representative images of the immunofluorescence of liver of Ad-CTRL and Ad-FAT10 fasted mice. Nuclear staining in blue with DAPI and FAT10 protein staining in red enhanced by tyramide detection. Central vein (CV) and portal triad (PT) are indicated. Scale bar: 50 µm. A graph showing *Fat10* relative mRNA expression measured by qPCR is associated. B) The Peroxisome proliferator-activated receptor α (*Pparα*) relative mRNA expression measured by qPCR. C) Correlation between *Fat10* and *Pparα* gene expression in total livers of fasted mice. The correlation is a linear regression, the p-value and correlation coefficient r are indicated. The best fit curve is shown with a line and the 95% confidence bands are represented with a dashed line. D) 3-hydroxy-3-methylglutaryl-CoA synthase 2 (*Hmgcs2*), Carnitine palmitoyltransferase 1 α (*Cpt1α*) and Acyl-CoA oxidase (*Aco*) mRNA relative expression measured by qPCR. E) Negative correlations between *Fat10* and *Pparα* expression, and between *Fat10* and Pparα target gene expression *Hmgcs2*, *Cpt1α*, Acyl-CoA dehydrogenase very long chain (*Acadvl*), Acyl-CoA dehydrogenase long chain (*Acadl*), Acyl-CoA dehydrogenase medium-chain (*Acadm*), *Aco*, Cytochrome P450 family 4 subfamily a polypeptide 10 (*Cyp4a10*) and Stearoyl CoA desaturase 1 (*Scd1*) in total livers of fasted mice. The correlations are linear regressions, the coefficient of correlation r and p-value are indicated. FAO: Fatty Acid Oxidation. TG: Triglyceride. F) Representative images of the proximity ligation assay (PLA) targeting FAT10 and PPARα proteins performed on liver sections of Ad-CTRL and Ad-FAT10 fasted mice by immunohistochemistry. Nuclear staining in blue with hematoxylin and FAT10-PPARα interaction detection in red. Images are represented full (scale bar: 50 µm) with a zoom on a selected representative zone (scale bar: 10 µm).

Values are mean ± SEM analyzed by two-way ANOVA (Ad-CTRL vs Ad-FAT10 $$$$ $p < 0.0001$, $$$ $p < 0.001$. Fed vs Fasted **** $p < 0.0001$, *** $p < 0.001$).

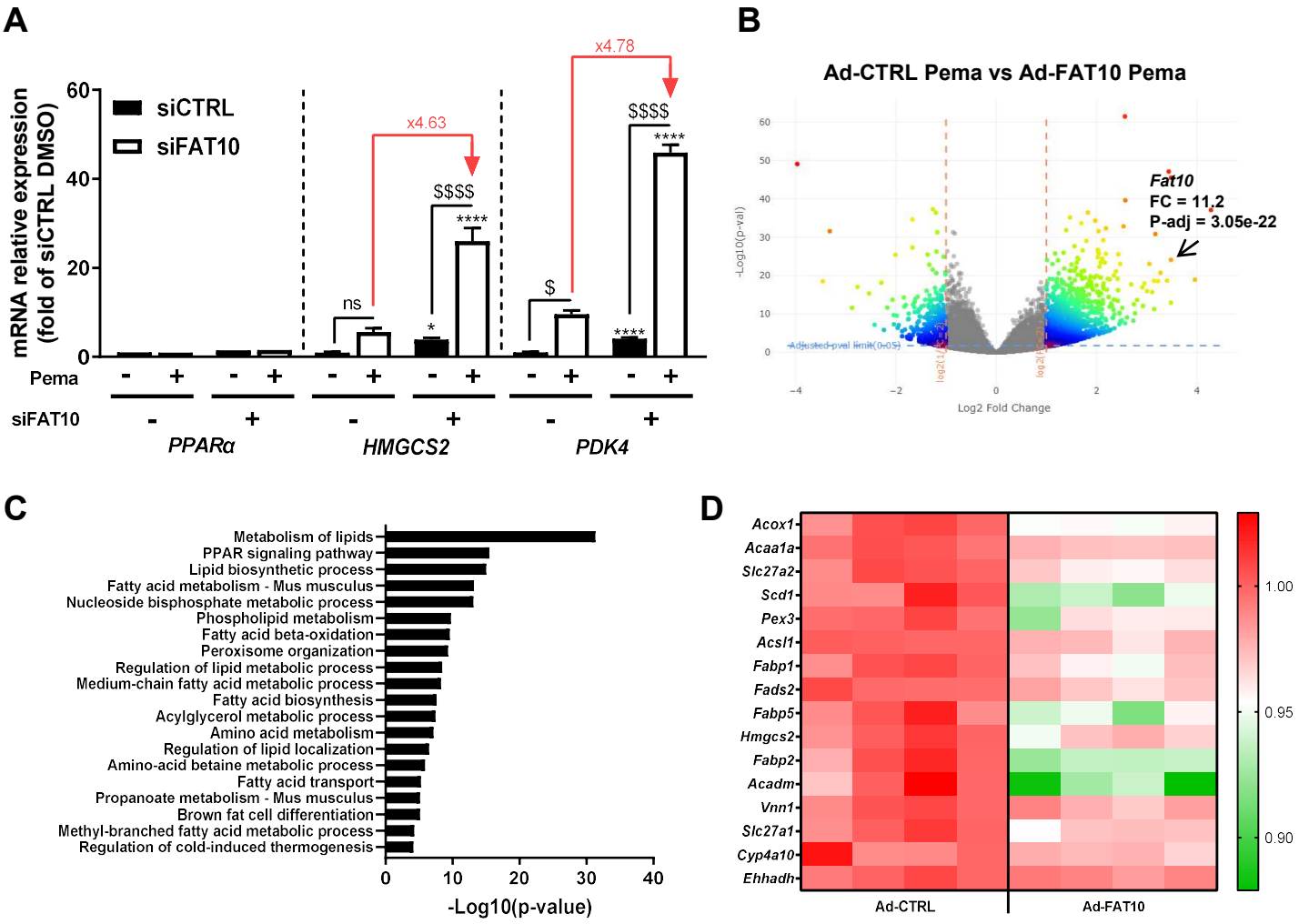
A
mRNA relative expression
(fold of siCTRL DMSO)
siCTRL
siFAT10
x4.63
x4.78
ns
*
$$$$
****
$
Pema
siFAT10
PPARα
HMGCS2
PDK4
B
Ad-CTRL Pema vs Ad-FAT10 Pema
Fat10
FC = 11.2
P-adj = 3.05e-22
-Log10(p-val)
Log2 Fold Change
C
Metabolism of lipids
PPAR signaling pathway
Lipid biosynthetic process
Fatty acid metabolism - Mus musculus
Nucleoside bisphosphate metabolic process
Phospholipid metabolism
Fatty acid beta-oxidation
Peroxisome organization
Regulation of lipid metabolic process
Medium-chain fatty acid metabolic process
Fatty acid biosynthesis
Acylglycerol metabolic process
Amino acid metabolism
Regulation of lipid localization
Amino-acid betaine metabolic process
Fatty acid transport
Propanoate metabolism - Mus musculus
Brown fat cell differentiation
Methyl-branched fatty acid metabolic process
Regulation of cold-induced thermogenesis
-Log10(p-value)
D
Acox1
Acaa1a
Slc27a2
Scd1
Pex3
Acsl1
Fabp1
Fads2
Fabp5
Hmgcs2
Fabp2
Acadm
Vnn1
Slc27a1
Cyp4a10
Ehhadh
Ad-CTRL
Ad-FAT10

Figure 6

Figure 6: Hepatic FAT10 modulation impairs the PPARα agonist response to lipid metabolism in vitro and in vivo.

HepG2 cells were transfected with a siRNA control (siCTRL) or a siRNA targeting the human Leukocyte antigen-F Adjacent Transcript 10 (FAT10) (siFAT10) during 24 h and then treated with human Tumor Necrosis Factor α (TNFα) (50 ng/mL) and Interferon γ (IFNγ) (10 ng/mL) (TNFα/IFNγ) during 24 more hours. The evening prior to the assay, cells were treated with 1 µM pemafibrate (Pema) or DMSO. A) The Peroxisome Proliferator-Activated Receptor α (*PPARα*), 3-hydroxy-3-methylglutaryl-CoA synthase 2 (*HMGCS2*) and Pyruvate Dehydrogenase 4 (*PDK4*) mRNA gene expression measured by qPCR and fold induction by Pema between siCTRL and siFAT10 are indicated with red arrows. Values are mean ± SD analyzed by two-way ANOVA (DMSO vs Pema: **** $p < 0.0001$, ** $p < 0.01$, * $p < 0.05$ with Pema fold induction indicated above the bars. siCTRL vs siFAT10 $$$$ $p < 0.0001$, $$$ $p < 0.001$, $ $p < 0.05$, ns $p > 0.05$). 8 week–old male mice were injected with a control adenovirus (Ad-CTRL) (N = 8) or adenovirus overexpressing FAT10 (Ad-FAT10) (N = 8) during 4 days. Then mice were orally treated with Pema at a total dose of 2 mpk (Ad-CTRL Pema N = 4 and Ad-FAT10 Pema N = 4) or control CMC (Ad-CTRL CMC N = 4 and Ad-FAT10 CMC N = 4): 1 mpk on the evening of the 4th day and 1 mpk on the morning of the 5th day. Then they were fasted during 5 h before livers were collected and analyzed by RNAseq. B) Volcano plot of total liver from Ad-CTRL vs Ad-FAT10 mice treated with Pema. C) Top enriched GO terms obtained by selecting the genes differentially expressed (p-value < 0.05) when comparing Ad-CTRL Pema vs Ad-FAT10 Pema and after applying a filter of the genes overexpressed by Pema treatment (the “UP Pema” filter i.e. genes significantly overexpressed (p-value < 0.05 and Fold Change (FC) > 1.5) when comparing Ad-CTRL CMC vs Ad-CTRL Pema). E) Heatmap comparing expressions of selected PPARα genes differentially expressed (p-value < 0.05) when comparing Ad-CTRL Pema vs Ad-FAT10 Pema.

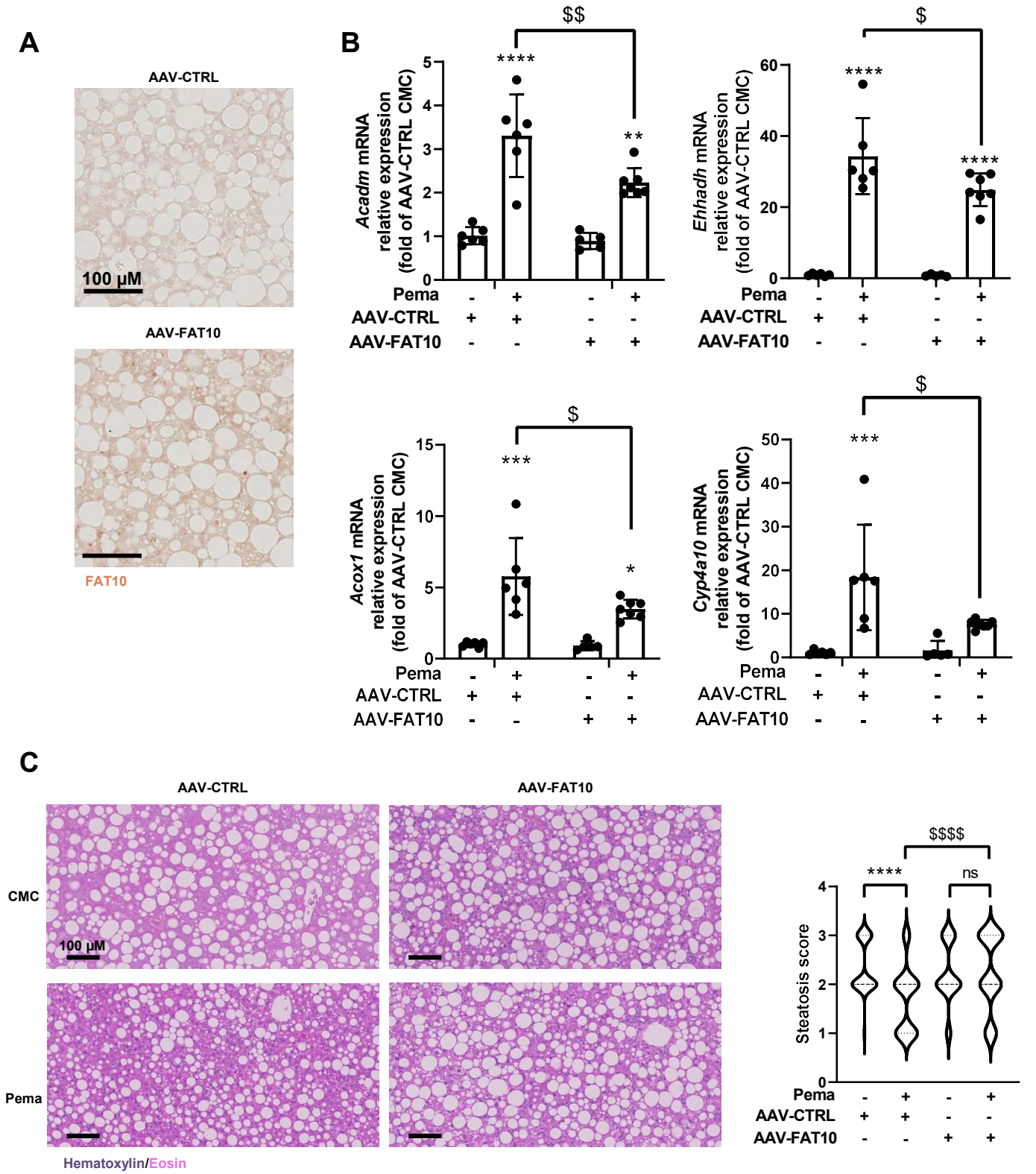
A
AAV-CTRL
100 µM
AAV-FAT10
FAT10
B
Acadm mRNA relative expression (fold of AAV-CTRL CMC)
Ehhadh mRNA relative expression (fold of AAV-CTRL CMC)
Acox1 mRNA relative expression (fold of AAV-CTRL CMC)
Cyp4a10 mRNA relative expression (fold of AAV-CTRL CMC)
Pema
AAV-CTRL
AAV-FAT10
C
AAV-CTRL
AAV-FAT10
CMC
Pema
100 µM
Hematoxylin/Eosin
Steatosis score
ns

Figure 7

Figure 7: Hepatocyte FAT10 overexpression inhibits the beneficial effect of PPARα agonist treatment on steatosis development in vivo.

12 week–old male mice were fed *ad libitum* with the choline deficient diet enriched with 1 % cholesterol, glucose and fructose (CDAA) during 2 weeks then injected with a control AAV (AAV-CTRL) (N = 12) or AAV overexpressing the human leukocyte antigen-F Adjacent Transcript 10 (FAT10) in hepatocytes (AAV-FAT10) (N = 12) and the diet was maintained for 3 more weeks. Then mice were orally treated with a total dose of 2 mpk of pemafibrate (Pema) (AAV-CTRL Pema N = 6 and AAV-FAT10 Pema N = 7) or control CMC (AAV-CTRL CMC N = 6 and AAV-FAT10 CMC N = 5): 1 mpk on the evening of the day preceding the sacrifice, and 1 mpk on the morning of the sacrifice. Then, mice were fasted during 5 h before livers were collected. A) Representative FAT10-Novared immunohistochemistry of livers of AAV-CTRL and AAV-FAT10 mice treated with CMC. Scale bar: 100 µm. B) Acyl-CoA dehydrogenase medium-chain (*Acadm*), Enoyl-CoA hydratase and 3-hydroxyacyl CoA dehydrogenase (*Ehhadh*), Cytochrome P450 family 4 subfamily a polypeptide 10 (*Cyp4a10*) and Acyl-CoA oxidase (*Aco*) mRNA relative expression measured by qPCR. C) Representative images of the Hematoxylin and Eosin staining performed on livers of AAV-CTRL and AAV-FAT10 mice treated with either CMC or Pema (scale bar: 100 µm), associated to a quantification of the steatosis scores determined on 10 Regions Of Interest (ROI) for each mouse and represented with a violin plot. Values are mean ± SEM (B) or ± SD (C) analyzed by two-way ANOVA (Pema vs CMC **** $p < 0.0001$, *** $p < 0.001$, ** $p < 0.01$, * $p < 0.05$ and AAV-CTRL vs AAV-FAT10 $$$$ $p < 0.0001$, $$ $p < 0.01$, $ $p < 0.05$, ns $p > 0.05$).

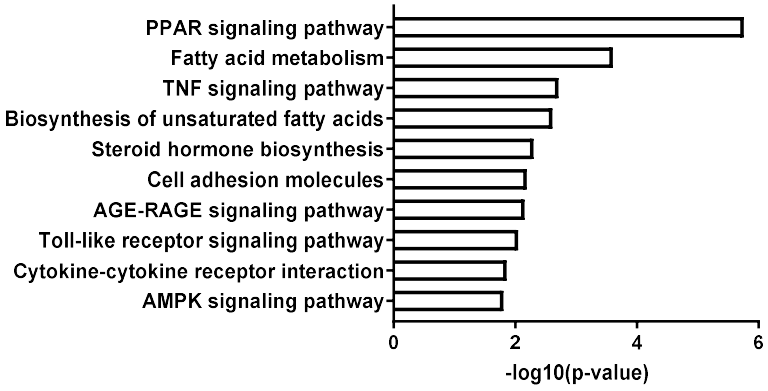

B

MASH vs no MASH

Gene	p-val	FDR.p-val	FC
LOC105369882	3.696e-09	1.939e-05	2.281
CDHR2	1.864e-08	4.139e-05	2.525
SRD5A2	1.913e-08	4.139e-05	2.268
CXCL10	7.486e-08	9.451e-05	2.293
SULF2	5.193e-07	0.0003745	2.194
IGFBP2	7.159e-07	0.0004367	0.3938
P4HA1	2.215e-06	0.0009067	0.382
SHBG	4.253e-06	0.001401	0.4016
PEG10	6.026e-06	0.001706	2.073
CXCL9	7.961e-06	0.002061	2.131
LOC101928635	9.205e-06	0.002296	2.328
LOC101927745	2.967e-05	0.004301	2.465
FAT10	**0.0001603**	**0.01181**	**2.388**
CRP	0.0007302	0.02954	2.22
SERPINE1	0.001089	0.03834	2.409
IGLC2	0.001802	0.05126	2.385
MT1H	0.002177	0.05734	2.037
LOC643675	0.002344	0.05987	0.3072
SPINK1	0.003363	0.07355	0.443

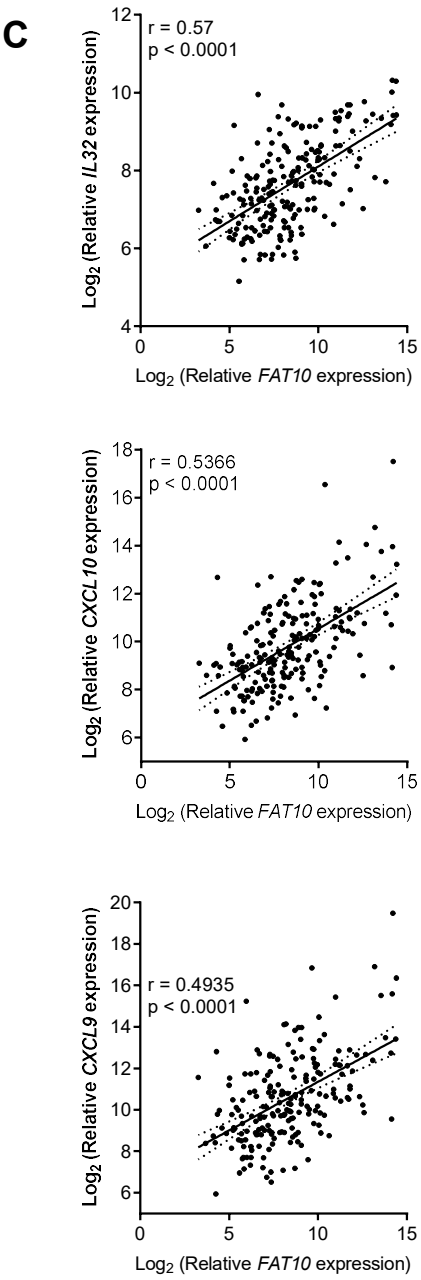

Supplementary Fig. 1: FAT10 is elevated in MASH patient livers and correlates positively with pro-inflammatory genes.

A) Gene ontology terms enrichment for genes in the livers of Metabolic-dysfunction Associated Steatohepatitis (MASH) patients vs no MASH patients. B) Top 20 genes enriched in the livers of MASH patients (N = 128) compared to no MASH (N = 77) C) Correlation between the human leukocyte antigen-F Adjacent Transcript 10 (FAT10) and the Interleukin 32 (*IL32*), the C-X-C motif chemokine ligand 10 and the C-X-C motif chemokine ligand 9 (*CXCL10* and *CXCL9*) gene expression. The correlations are linear regressions, the p-values and the correlation coefficient r are indicated. The best fit curve is shown with a line and the 95% confidence bands are represented with a dashed line.

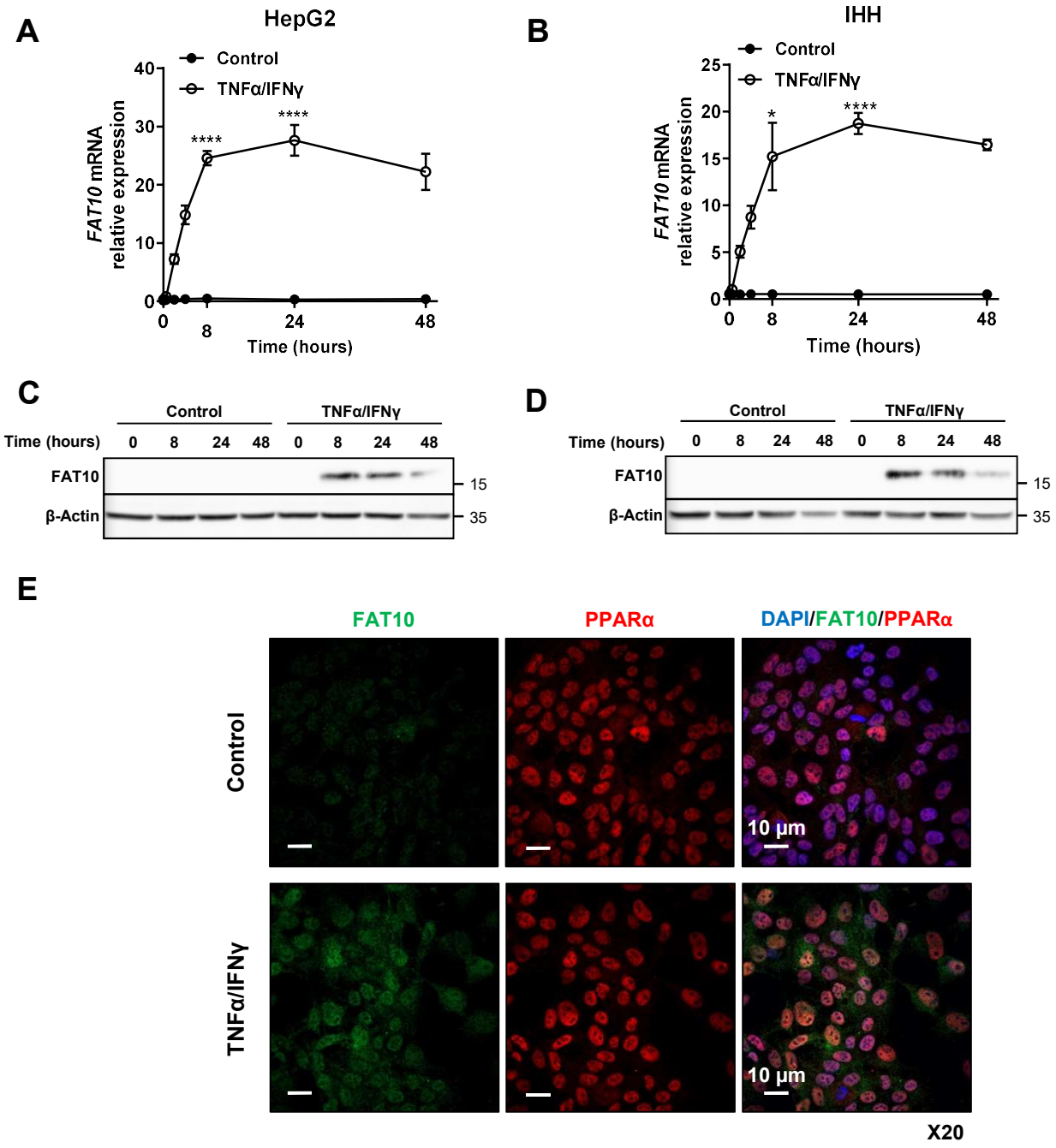

Supplementary Fig. 2: FAT10 is induced by cytokines in hepatocytes and colocalizes with PPARα.

The human leukocyte antigen-F Adjacent Transcript 10 (*FAT10*) mRNA gene expression measured by qPCR over time for A) HepG2 cells or B) Immortalized Human Hepatocytes (IHH) cells treated with human Tumor Necrosis Factor α (TNFα) (50 ng/mL) and Interferon γ (IFNγ) (10 ng/mL) (TNFα/IFNγ) or untreated (Control). Values are mean ± SD analyzed by two-way ANOVA (**** $p < 0.0001$, * $p < 0.5$). Western blot for FAT10 in C) HepG2 and D) IHH cells treated with TNFα/IFNγ or untreated (Control) as described before. β-Actin protein expression is used as a loading control. E) Immunofluorescence of HepG2 cells treated or not with TNFα/IFNγ during 24 h. Nuclear staining in blue with DAPI, FAT10 protein staining in green and the Peroxisome Proliferator-Activated Receptor α (PPARα) protein staining in red. Scale bar: 10 µm.

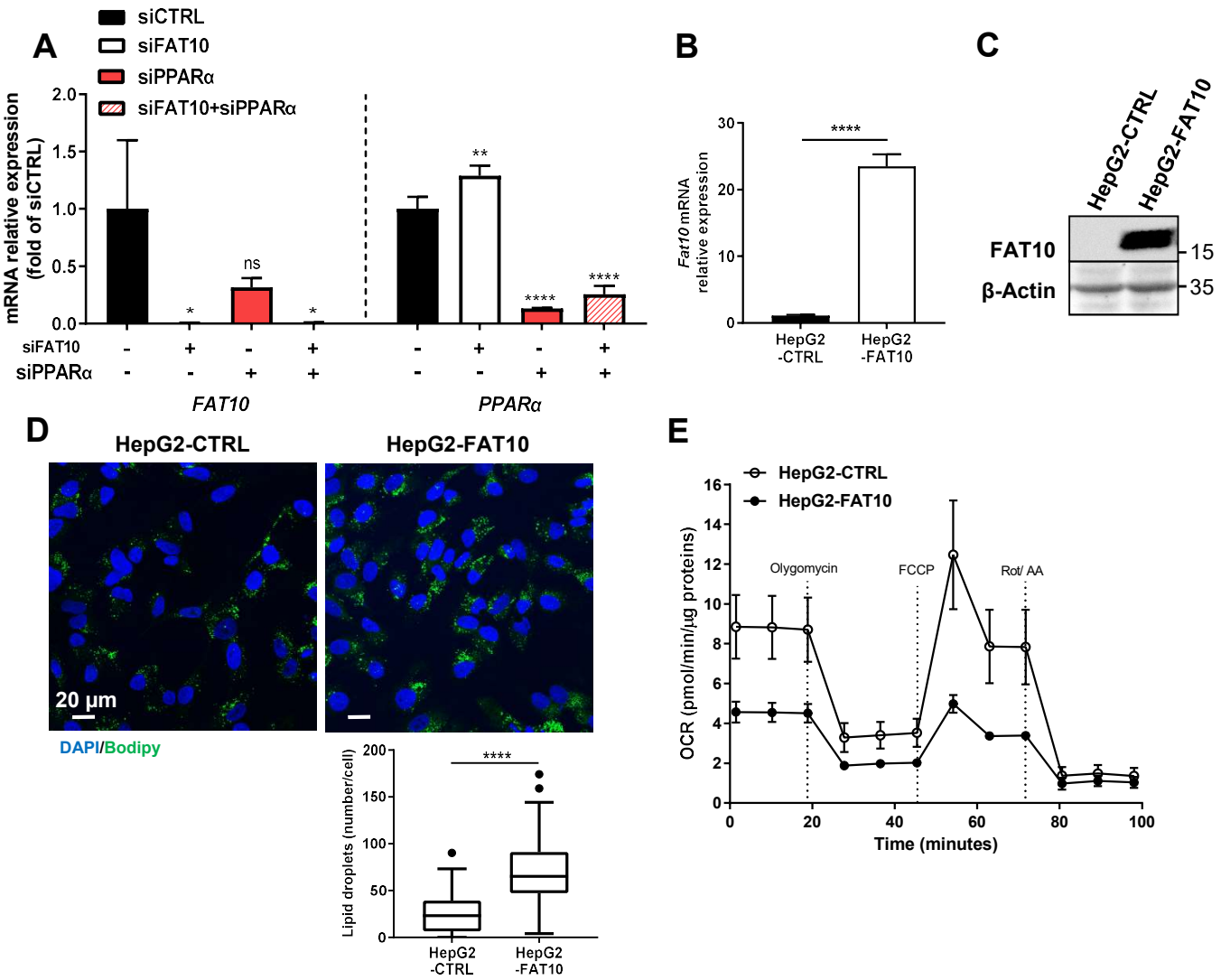

Supplementary Fig. 3: FAT10 overexpressing cells accumulate lipid droplets and have an impaired mitochondrial respiration.

HepG2 cells were transfected with a siRNA control (siCTRL) or a siRNA targeting the human leukocyte antigen-F Adjacent Transcript 10 (FAT10) (siFAT10) with or without a siRNA targeting the Peroxisome Proliferator-Activated Receptor α (PPARα) (siPPARα) during 24 h and then treated with human Tumor Necrosis Factor α (TNFα) (50 ng/mL) and Interferon γ (IFNγ) (10 ng/mL) (TNFα/IFNγ) during 24 more hours. A) *FAT10* and *PPARα* mRNA gene expression measured by qPCR. Values are mean ± SD analyzed by two-way ANOVA (siCTRL vs siRNA: **** $p < 0.0001$, *** $p < 0.001$, ** $p < 0.01$, * $p < 0.05$, ns non-significant). HepG2 cells overexpressing stably FAT10 were obtained after an infection with a lentivirus FAT10 (HepG2-FAT10) or a lentivirus control (HepG2-CTRL) as described in methods. B) *FAT10* mRNA expression measured by qPCR and C) FAT10 protein expression measured by western Blot. β-Actin protein expression is used as a loading control. D) Representative images of BODIPY 493/503 staining of neutral lipids (scale bar: 20 µm) with the quantification of lipid droplets per cell using the spot detection plug-in of the Icy software. E) Oxygen Consumption Rate (OCR) in HepG2-FAT10 or HepG2-CTRL cells incubated for 1 h in Seahorse assay media complemented with 1 mM pyruvate, 2 mM glutamine, and 10 mM glucose. OCR was measured over time after treatment with Oligomycin (2 µM), ATP synthase inhibitor; FCCP (1 µM), mitochondrial uncoupler; and rotenone and antimycin A (Rot/AA) (0.5 µM), specific inhibitors for ETC complex I and III, respectively. Values are mean ± SD analyzed by two-way ANOVA (siCTRL vs siRNA or HepG2-CTRL vs HepG2-FAT10 **** $p < 0.0001$, ** $p < 0.01$, * $p < 0.05$, ns non-significant).

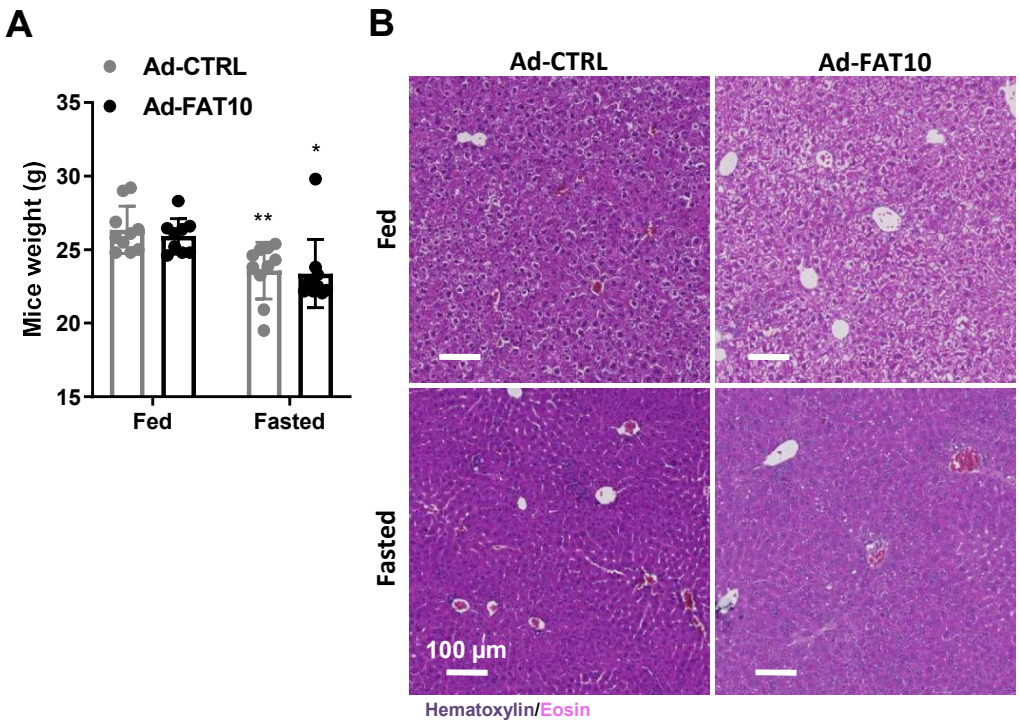

Supplementary Fig. 4: Hepatic FAT10 overexpression does not affect mice body weight or liver histology.

8 week–old male mice were injected with a control adenovirus (Ad-CTRL) (N = 20) or adenovirus overexpressing the human leukocyte antigen-F Adjacent Transcript 10 (FAT10) (Ad-FAT10) (N = 19) during 4 days. Then mice were fed *ad libitum* (Ad-CTRL fed N = 10, Ad-FAT10 fed N = 9) or fasted during 18 h (Ad-CTRL fasted N = 10, Ad-FAT10 fasted N = 10) before livers were taken. A) Mice body weight. B) Representative images of hematoxylin and eosin immunohistochemistry on mice livers for each group. Scale bar: 100 µm. Values are mean ± SEM analyzed by two-way ANOVA (Fed vs Fasted ** $p < 0.01$, * $p < 0.05$).

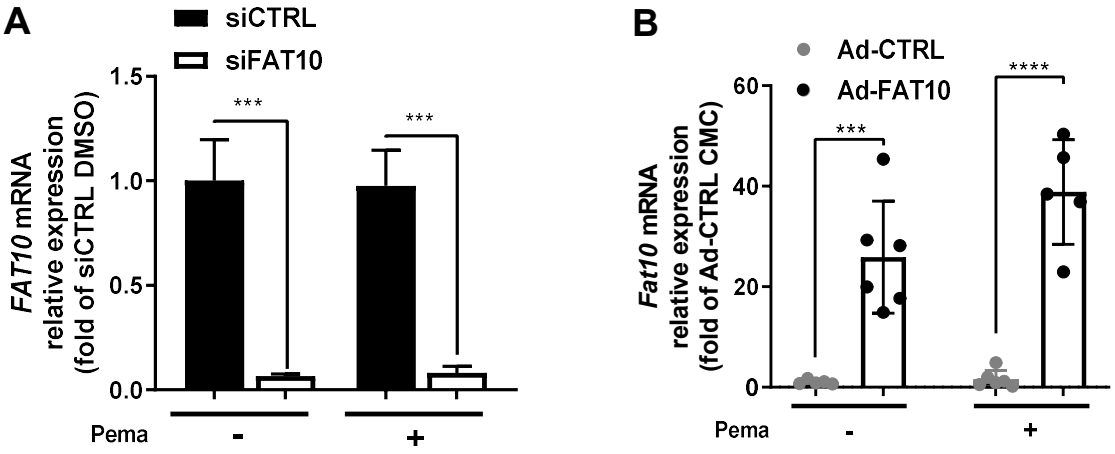

Supplementary Fig. 5: FAT10 expression is not modulated by pemafibrate treatment neither *in vitro* nor *in vivo*.

HepG2 cells were transfected with a siRNA control (siCTRL) or a siRNA targeting the human leukocyte antigen-F Adjacent Transcript 10 (FAT10) (siFAT10) during 24 hours and treated with human Tumor Necrosis Factor α (TNFα) (50 ng/mL) and Interferon γ (IFNγ) (10 ng/mL) (TNFα/IFNγ) during 24 more hours. The evening prior to the assay, cells were treated with 1 µM pemafibrate (Pema) or DMSO. A) *FAT10* mRNA expression measured by qPCR. Values are mean ± SD analyzed by two-way ANOVA (*** $p < 0.001$). B) *Fat10* mRNA expression measured by qPCR in the livers of 8 week–old male mice injected with a control adenovirus (Ad-CTRL) (N = 11) or adenovirus overexpressing FAT10 (Ad-FAT10) (N = 11) during 4 days. This mice were orally treated with 1 mpk Pema (Ad-CTRL Pema N = 6 and Ad-FAT10 Pema N = 5) or control CMC (Ad-CTRL CMC N = 5 and Ad-FAT10 CMC N = 6) on the evening of the 4th day and the morning of the 5th day. Then mice were fasted during 5 h before livers were taken. Values are mean ± SEM analyzed by two-way ANOVA (Ad-CTRL vs Ad-FAT10 **** $p < 0.0001$, *** $p < 0.001$).

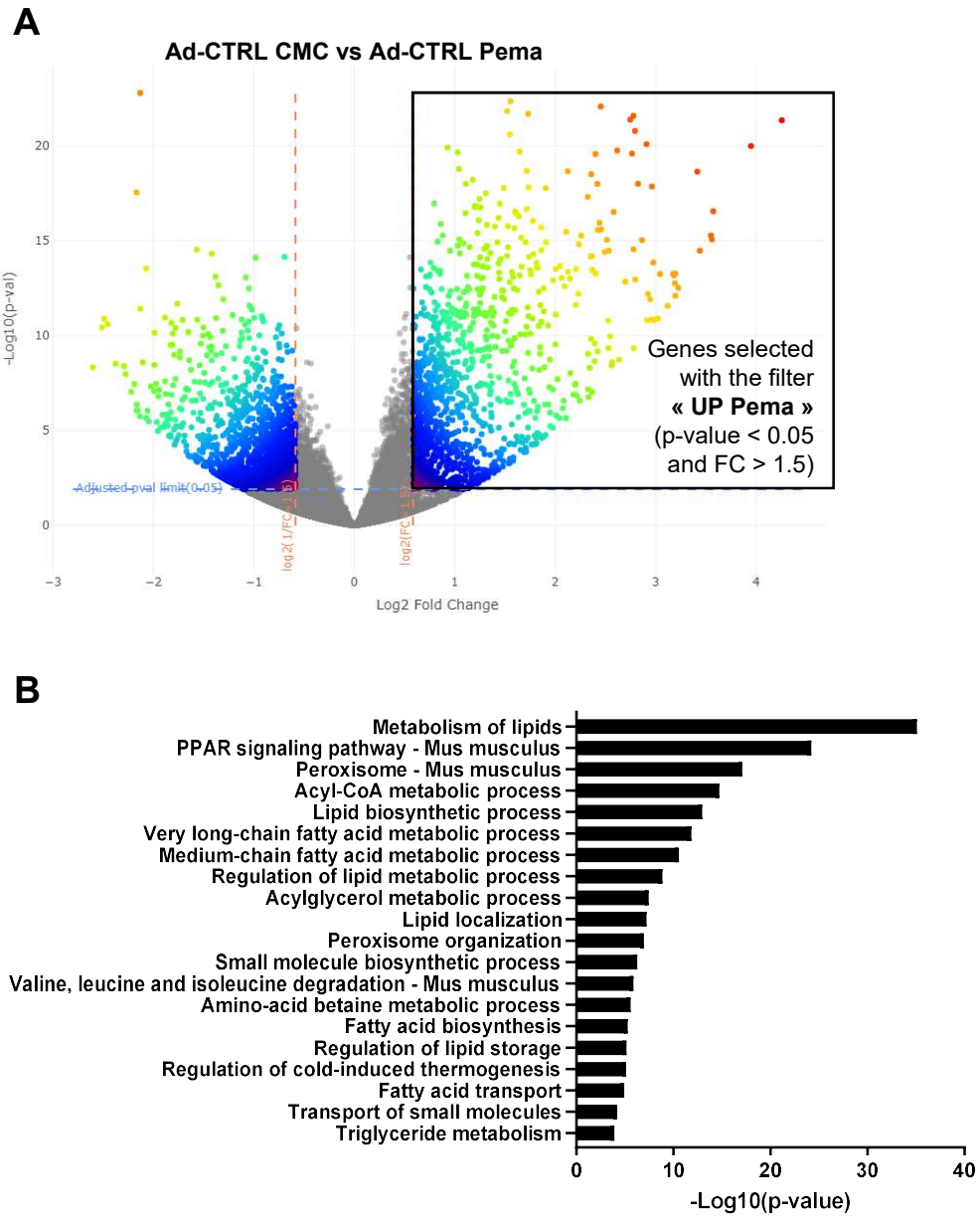

Supplementary Fig. 6: Genes differentially expressed by pemafibrate treatment on Ad-CTRL mice.

8 week–old male mice were injected with a control adenovirus (Ad-CTRL) (N = 8) during 4 days. Then mice were orally treated with 1mpk of pemafibrate (Pema) (Ad-CTRL Pema N = 4) or control CMC (Ad-CTRL CMC N = 4) on the evening of the 4th day and 1 mpk on the morning of the 5th day. Then they were fasted during 5 h before livers were collected and analyzed by RNAseq. A) Volcano plot of total liver from Ad-CTRL mice treated with CMC vs Ad-CTRL mice treated with Pema. The black square indicates the genes selected for the determination of the « UP Pema » filter i.e. genes significantly overexpressed (p-value < 0.05 and FC > 1.5) when comparing Ad-CTRL CMC vs Ad-CTRL Pema. B) Gene ontology terms enrichment for genes of the UP Pema filter.

The ubiquitin-like modifier FAT10 is induced in MASLD and impairs the lipid regulatory activity of PPARα

Ludivine Clavreul*, Lucie Bernard*, Alexia K. Cotte, Nathalie Hennuyer, Cyril Bourouh, Claire Devos, Audrey Helleboid, Joel T. Haas, An Verrijken, Céline Gheeraert, Bruno Derudas, Loïc Guille, Julie Chevalier, Jérôme Eeckhoute, Emmanuelle Vallez, Emilie Dorchies, Luc Van Gaal, Guillaume Lassailly, Sven Francque, Bart Staels+, Réjane Paumelle+#

* Co-first authors

+ Co-senior authors

Corresponding author: rejane.lestrelin@univ-lille.fr

12. Supplemental methods

12.1 Human and liver samples

For the immunofluorescence assays, biopsies were selected amongst the cohort according to histological parameters: 5 control patients (steatosis, inflammation, ballooning and fibrosis = 0) and 10 MASH patients (steatosis > 1 or 5 %, inflammation ≥ 1, ballooning ≥ 2 and fibrosis ≤ 3 [1]) were selected.

12.2 Transcriptomics

Anthropometric, histological and metabolic characteristics, RNA extraction, purification, labelling and hybridization procedures have been previously reported [2]. Transcriptome analysis was performed using Affymetrix Human Gene (HuGene) 2.0ST and .CEL files were normalized as above. Gene Expression Omnibus (GEO) repository accession numbers are for microarray data GSE212617 and for RNA-sequencing data

GSE239392. The correlations were calculated with the Pearson tests. Data handling was performed using the GIANT module and the RNA-SEQ ANALYSIS module on Galaxy tool (Galaxy tool ID : testtoolshed.g2.bx.psu.edu/repos/vandelj/giant_gsea_format/giant_gsea_format/0.2.0; Galaxy Version 0.2.0; Normalization: NetAffx Annotation Release 36, July 2016) [3–9].

12.3 RNA extraction and quantitative real-time PCR

Trizol reagent was used to extract total messenger RNA (mRNA) from cells and tissues. The mRNA samples were then reverse transcribed into complementary DNA (cDNA) according manufacturer's protocol of the kit (Applied Biosystems, Thermofischer Scientific). Then, mRNA expression was assessed with a real-time qPCR using SYBR Green PCR Master Mix or TaqMan PCR Master Mix and the normalization was made with the respective housekeeping genes Cyclophilin and β-actin. The primers and probes are listed in Supplementary table 1.

12.4 Western blot analysis

Cells were gathered in PBS and resuspended in RIPA buffer containing PMSF and phosphatase inhibitor after centrifugation at 400 g for 10 min and lysed for 10 more minutes on ice. BCA kit was then used to assess the protein concentration of these samples. 40 µg of proteins were denatured with Laemmli buffer, subjected to 10 % or 12 % SDS-PAGE and transferred onto a nitrocellulose membrane. Primary antibodies, listed in the Supplementary table 2, were diluted in TBS supplemented with 0.01 % of tween and 5 % of powder milk and used to incubate the membranes overnight at 4 °C. The corresponding secondary antibodies were then incubated for 1 h at room

temperature and chemiluminescence signals were detected thanks to Dura detection kit on the IBright.

12.5 Cell lines and cell culture

The human cell line HepG2 (cat. no. HB-8065, ATCC) was cultured in Minimum Essential Medium (MEM, 11095080, GIBCO) supplemented with 10 % FBS, MEM Non-essential Amino Acids (NEAA, 11140035, GIBCO) and sodium pyruvate (11360070, GIBCO). The human cell line IHH was cultured in William's E Medium (22551022, GIBCO) supplemented with 10 % FBS, 20 mU/mL of bovine insulin (I5500, Sigma) and 50 nM of dexamethasone (D1756, Sigma). They were both kept in a humidified atmosphere of 5 % CO_2 in a 37 °C incubator.

12.6 Cell transfection, stimulation, and lentivirus

IHH and HepG2 cells were transfected with siRNA targeting FAT10 (Smart pool siGENOME UBD) or a siRNA control (siCTRL, Horizon Discovery) using the Dharmafect (Horizon Discovery) reagent according to the manufacturer's instructions. Primary murine hepatocytes, or HepG2 and IHH cells 24h after siRNA transfection, were respectively treated or not with a cocktail of 50 ng/mL of murine TNFα (410-MT-025, eBioscience) or human TNFα (BMS301, eBioscience), and 10 ng/mL of murine IFNγ (485-MI-100, eBioscience) or human IFNγ (RIFNG50, Thermo Scientific) to induce endogenous FAT10. After 40h of siRNA transfection and/or 16h of cytokines treatments, cells were treated with 1 µM of pemafibrate during 8 more hours.

For the overexpression of FAT10 in HepG2 cells, the lentiviral vectors containing FAT10-MykDDK tagged vector and the gene to resistance to puromycin were

purchased from Origene. HepG2 cells were infected with these particles in HepG2 medium and in presence of polybrene during 48 hours. Then, the cells were selected by treatment with 0.5 µM puromycin.

12.7 Seahorse analysis

Measurements of oxygen consumption rate (OCR) were performed using the XFe24 apparatus (Seahorse Bioscience, North Billerica, MA). Cells were plated into XFe24 (V7) polystyrene culture plates (Seahorse Bioscience, North Billerica) at 70 000 cells/well (XFe24 plate). The cells were incubated for 24h and transfected, if needed, with siRNA for 48h as previously described. Sensor cartridges were calibrated prior to each assay. Then, the cells incubated for 1h in complete Seahorse assay medium (10 mM Glucose, 2mM Glutamine) in a 37 °C/non-CO2 incubator before the start of the assay. All experiments were performed at 37 °C. Each cycle of measurement was design as follow: a mixing time of 3 min, a waiting time of 2 min and a data acquisition period of 3 min. OCR data points represent to the average rates during the measurement cycles. Oligomycin, FCCP and Rotenone/Antimycin A were prepared at respectively 2 µM, 1 µM and 0.5 µM.

12.8 BODIPY 493/503 staining

Cells seeded on coverslips were fixed in 4 % PFA for 10 min at 4 °C and incubated with Bodipy 493/503 (Molecular Probes) at 200 ng/mL and NucBlue (Invitrogen) for 20 min at room temperature. Cells were mounted in fluorescent mounting medium (Dako). Acquisitions were performed using an inverted confocal microscope (Spinning Disk, Zeiss) with 40X oil immersion lens (NA 1.3 with an optical resolution of 176 nm) and 1.8X digital zoom or a dry 20X lens. Bodipy and NucBlue fluorescence were imaged

using argon 488 nm and UV lasers, respectively. Images were processed with Zen and analyzed with Icy programs.

12.9 Immunofluorescence

Cells seeded on glass coverslips previously coated with polylysine were washed with cold PBS and fixed with 4 % paraformaldehyde (PFA) for 10 min at 4 °C. Cells were permeabilized and blocked with a solution containing 1 % of Bovine Serum Albumin (BSA) and 0.2 % Triton X-100 in PBS at room temperature for 30 min. Cells were then incubated overnight at 4 °C with the following primary antibodies: FAT10 (LS Bio, LS-C166057) and PPARα (Santa Cruz, sc-398394) in blocking solution (see Supplementary table 2). Then, cells were washed and incubated 1 h at room temperature with secondary antibodies coupled respectively to Alexa 488 and Alexa 594 (Molecular Probes by Life technologies) diluted in blocking solution containing NucBlue (Invitrogen). Cells were mounted in fluorescence mounting medium (Dako).

Human or murine liver biopsy sections were incubated overnight at 4 °C with a primary antibody anti-FAT10 (described before). Then, human or murine tissues were respectively incubated with Alexa fluor 488 or Alexa fluor 594 Tyramide SuperBoost anti-rabbit antibody, and revealed as indicated by the supplier (Thermofischer Scientific). Sections were then incubated 20 min with a solution of NucBlue (Invitrogen) in PBS during 20 min before being mounted in fluorescence mounting medium (Dako).

Acquisition for immunofluorescence were performed using an inverted confocal microscope (Spinning disk, Zeiss) with a 40X oil-immersion lens (NA 1.3 with an optical resolution of 176 nm) or a slide scanner microscope Axio Scan, Z1 (Zeiss) with a 20X dry lens (NA 0.8). Alexa 594, Alexa 488 and NucBlue were imaged using UV, argon 488 nm and 561 nm lasers.

Images were processed with Zen software and analyzed with Icy software.

12.10 Immunohistochemistry

Murine liver biopsy sections were incubated overnight at 4 °C with a primary antibody directed against FAT10 (LS Bio, LS-C166057) (see Supplementary table 2). Then, anti-rabbit secondary antibody coupled with HRP was added, and mice liver sections were incubated with the Novared reagent, according to manufacturer's instructions (Vector Immpress). Sections were then mounted in Eukitt mounting medium (VWR) and images of the full slides were taken with an axioscan (Zeiss), before being analysed with Zen software.

12.11 Proximity Ligation Assay

Proximity Ligation Assay (PLA) was performed on cells and tissues with the same primary antibodies for FAT10 and PPARα (mentioned before) as indicated by the supplier (Sigma) (see Supplementary table 2).

Images were acquired using an inverted confocal microscope (Spinning disk, Zeiss) with a 40X oil-immersion lens as described before.

12.12 Histological analysis

Mouse liver samples were fixed with 4 % PFA, embedded in paraffin and stained with hematoxylin and eosin. Images were obtained using a slide scanner microscope Axio Scan, Z1 (Zeiss) with a X20 dry lens (NA 0.8).

The NAS score was obtained by adding the scores for steatosis, inflammation and ballooning determined by visual analyses of the tissues [1].

The steatosis score (0 for a percentage of steatosis (S) < 5 %, 1 for 5 % < S < 33 %, 2 for 33 % < S < 66 %, 3 for S > 66 %) was established on 10 ROI (region of interest) selected randomly on the liver of each mouse and analyzed in double-blind.

12.13 Co-Immunoprecipitations (Co-IP) assay

HepG2 and IHH cells were treated with recombinant cytokines as described before to induce endogenous FAT10. They were lysed in ice cold IP buffer provided in the kit (88805, Thermofischer Scientific). The cell lysates were then incubated with the FAT10 antibody (Millipore), which was beforehand conjugated to magnetic beads, at 4 °C overnight. After that, proteins conjugated to the beads were eluted and subjected to western blot assays as described before (see Supplementary table 2).

12.14 Supplementary table 1: Primers and probes

Gene	Species	Sequence	
Cyclophilin	Human/ Mouse	Forward	GCATACGGGTCCTGGCATCTTGTCC
		Reverse	ATGGTGATCTTCTTGCTGGTCTTGC
FAT10	Human	Forward	CAGAGATGGCTCCCAATGCT
		Reverse	TTGGGAAATCATCAGAAGAT
Fat10	Mouse	Forward	TTCTGTCCGCACCTGTGTTG
		Reverse	TGCCCCTCGTTTTTGGACTC
PPARα	Human	Forward	GGTGGACACGGAAAGCCCAC
		Reverse	GGACCACAGGATAAGTCACC
Pparα	Mouse	Forward	ATCGCGTACGGCAATGGCTTTA
		Reverse	CAGGCCGATCTCCACAGCAAATTA
HMGCS2	Human	Forward	AGGCTGGAAGTAGGCACTGA
		Reverse	GTGGGACGAGCATTACCACT
Hmgcs2	Mouse	Forward	TGGCCATGTATCTGTTTTGG
		Reverse	TGCAAGTGAAGAGAGCGATG
PDK4	Human	Forward	GATGAACCAGCACATTCTTA
		Reverse	GCTACCACATCACAGTTAGG
Cpt1α	Mouse	Forward	TGGTTAACAGCAACTACTACG
		Reverse	GACGAATAGGTTTGAGTTCC

Acadvl	Mouse	Forward	CTCAGTGAAGAACAGGCACAA
		Reverse	CTT GGC AGG GTC ATT CAC TT
Acadl	Mouse	Forward	ATC TTT TCC TCG GAG CAT GA
		Reverse	TTT CTC TGC GAT GTT GAT GC
Acadm	Mouse	Forward	GCC CAG AGA GCT CTA GAC GA
		Reverse	CCA GGC TGC TCT CTG GTA AC
Aco	Mouse	Forward	ACG TCT TGG ATG GTA GTC CG
		Reverse	TAA CGC TGG CTT CGA GTG AG
Acox1	Mouse	Forward	AGACGGCCAGGTTCTTGATG
		Reverse	GACACCATACCACCCACCAG
Cyp4a10	Mouse	Forward	TGA GGG AGA GCT GGA AAA GA
		Reverse	CTG TTG GTG ATC AGG GTG TG
Cyp4a14	Mouse	Forward	TTGCTCACGAGCACACAGAT
		Reverse	TCCTCCATTCTGGCAAACAAGA
Ehhadh	Mouse	Forward	TTGCCAATGCAAAGGCTCGT
		Reverse	GCAACAGGAACTCCAACGAC
Scd1	Mouse	Forward	TTCCCTCCTGCAAGCTCTACACCTG
		Reverse	AGCCGTGCCTTGTAAGTTCTGTGG

12.15 Supplementary table 2: Antibodies

Protein (clone)	Application	Reference
β-actin (AC15)	WB	Sigma (A5441)
HSP90 (H-114)	WB	Santa Cruz (Sc-8303)
PPARα (H2)	WB, IF, PLA	Santa Cruz (sc-398394)
FAT10 (4F1)	WB, CoIP	Millipore (MABS351)
FAT10	IF, PLA	LS Bio ((LS-C334091)
DDK (OTI4C5)	WB	Origene (TA50011)

12.16 Supplementary table 3: no MASH and MASH patients' biological parameters

Total - 205 patients	no MASH - 77 patients		MASH - 128 patients	
	Sex ratio M/F: 0.21		Sex ratio M/F: 0.43	
	Mean	Standard deviation	Mean	Standard deviation
Age (years old)	43.43	12.99	44.59	13.29
BMI (kg/m²)	33.81	6.82	39.25	5.87
ASAT (U/L)	23.40	10.45	28.31	19.39
ALAT (U/L)	57.08	33.24	49.23	31.79
GGT (U/L)	19.24	26.08	43.81	42.11
Total cholesterol (mg/dL)	128.86	84.93	176.13	66.23
HDL-cholesterol (mg/dL)	80.83	46.74	66.06	58.75
TG (mg/dL)	124.30	56.22	162.49	75.96
LDL-cholesterol (mg/dL)	100.27	38.92	116.71	31.71
HBA1c (%)	5.34	0.29	5.62	0.59
HOMA-IR	2.38	1.68	4.76	5.78
CRP (mg/dL)	0.50	0.62	0.60	0.61

13. Supplemental references

[1] Kleiner DE. Brunt EM. Van Natta M. Behling C. Contos MJ. Cummings OW. et al. Design and validation of a histological scoring system for nonalcoholic fatty liver disease. Hepatology 2005;41:1313–21. https://doi.org/10.1002/hep.20701.

[2] **Francque S**. **Verrijken A**. Caron S. Prawitt J. Paumelle R. Derudas B. et al. PPARa gene expression correlates with severity and histological treatment response in patients with Non-Alcoholic Steatohepatitis. J Hepatol 2015. https://doi.org/10.1016/j.jhep.2015.02.019.

[3] Vandel J. Gheeraert C. Staels B. Eeckhoute J. Lefebvre P. Dubois-Chevalier J. GIANT: galaxy-based tool for interactive analysis of transcriptomic data. Sci Rep 2020;10:1–13. https://doi.org/10.1038/s41598-020-76769-w.

[4] Galili T. O'Callaghan A. Sidi J. Sievert C. Heatmaply: An R package for creating interactive cluster heatmaps for online publishing. Bioinformatics 2018;34:1600–

2. https://doi.org/10.1093/bioinformatics/btx657.

[5] Gu Z. Gu L. Eils R. Schlesner M. Brors B. Circlize implements and enhances circular visualization in R. Bioinformatics 2014;30:2811–2. https://doi.org/10.1093/bioinformatics/btu393.

[6] Subramanian A. Tamayo P. Mootha VK. Mukherjee S. Ebert BL. Gillette MA. Paulovich A. Pomeroy SL. Golub TR. Lander ES MJ. Gene set enrichment analysis: A knowledge-based approach for interpreting genome-wide expression profiles. Proc Natl Acad Sci 2005;102:15545--15550. https://doi.org/10.3969/j.issn.0372-2112.2018.08.016.

[7] Ritchie ME. Phipson B. Wu D. Hu Y. Law CW. Shi W. et al. Limma powers differential expression analyses for RNA-sequencing and microarray studies. Nucleic Acids Res 2015;43:e47. https://doi.org/10.1093/nar/gkv007.

[8] Scientific TF. Affymetrix Power Tools. 2018. https://www.affymetrix.com/support/developer/powertools/changelog/index.html .

[9] Inc. PT. Collaborative data science 2015. https://plot.ly/.